Mon. Not. R. Astron. Soc. **000**, 1–?? (2015) Printed 27 October 2015 (MN LATEX style file v2.2)

H ingestion into He-burning convection zones in super-AGB stellar models as a potential site for intermediate neutron-density nucleosynthesis

S. Jones[1,2,†⋆], C. Ritter[1,3,†], F. Herwig[1,3,†], C. Fryer[4,†], M. Pignatari[5,†], M. G. Bertolli[6,7,†,‡] and B. Paxton[8]

[1] *Department of Physics & Astronomy, University of Victoria, P.O. Bos 3055 Victoria, B.C., V8W 3P6, Canada*
[2] *Heidelberg Institute for Theoretical Studies, Schloss-Wolfsbrunnenweg 35, D-69118 Heidelberg, Germany*
[3] *Joint Institute for Nuclear Astrophysics, Center for the Evolution of the Elements, Michigan State University 640 South Shaw Lane, East Lansing, MI 48824, USA*
[4] *Computational Physics and Methods (CCS-2), LANL, Los Alamos, NM, 87545, USA*
[5] *Konkoly Observatory, Research Centre for Astronomy and Earth Sciences, Hungarian Academy of Sciences, Konkoly-Thege Miklós ut 15-17, H-1121 Budapest, Hungary*
[6] *Physics Division, Oak Ridge National Laboratory, Oak Ridge, Tennessee 37831, USA.*
[7] *Department of Physics and Astronomy, University of Tennessee, Knoxville, Tennessee 37996, USA*
[8] *Kavli Institute for Theoretical Physics and Department of Physics Kohn Hall, University of California, Santa Barbara, CA 93106, USA*
[†] *NuGrid Collaboration,* http://www.nugridstars.org
[‡] *Formerly LANL*

arXiv:1510.07417v1 [astro-ph.SR] 26 Oct 2015

Submitted: June 2015

ABSTRACT

We investigate the evolution of super-AGB thermal pulse (TP) stars for a range of metallicities (Z) and explore the effect of convective boundary mixing (CBM). With decreasing metallicity and evolution along the TP phase, the He-shell flash and the third dredge-up (TDU) occur closer together in time. After some time (depending upon the CBM parameterisation), efficient TDU begins while the pulse-driven convection zone (PDCZ) is still present, causing a convective exchange of material between the PDCZ and the convective envelope. This results in the ingestion of protons into the convective He-burning pulse. Even small amounts of CBM encourage the interaction of the convection zones leading to transport of protons from the convective envelope into the He layer. H-burning luminosities exceed 10^9 (in some cases 10^{10}) $L_\odot$. We also calculate models of dredge-out in the most massive super-AGB stars and show that the dredge-out phenomenon is another likely site of convective-reactive H-^{12}C combustion. We discuss the substantial uncertainties of stellar evolution models under these conditions. Nevertheless, the simulations suggest that in the convective-reactive H-combustion regime of H-ingestion the star may encounter conditions for the intermediate neutron capture process (*i* process). We speculate that some CEMP-s/r stars could originate in i-process conditions in the H-ingestion phases of low-Z SAGB stars. This scenario would however suggest a very low electron-capture supernova rate from super-AGB stars. We also simulate potential outbursts triggered by such H-ingestion events, present their light curves and briefly discuss their transient properties.

Key words: stars: AGB and post-AGB — abundances — evolution — interior

1 INTRODUCTION

The most important mixing process in stars is convection. One of the least-understood aspects of stellar convection is the convective boundary. The way in which convective boundaries are modelled determines many global properties that characterise the evolution of stellar models. In the most simplistic view the convective boundary is given by the Schwarzschild condition ($\nabla_{\rm rad} > \nabla_{\rm ad}$). However, the literal implementation of the Schwarzschild boundary would imply a spherically symmetric composition discontinuity that does not exist in real stars, as shown by hydrodynamic simulations and observations (see, e.g. Freytag, Ludwig & Steffen 1996; Schroder, Pols & Eggleton 1997; Deupree 2000; Ribas, Jordi & Gimenez 2000; Herwig et al. 2006; Rogers, Glatzmaier & Jones 2006; Meakin & Arnett 2007; Herwig et al. 2007; Woodward et al.

⋆ Email: samuel.jones@h-its.org

© 2015 RAS

2008; Mocák et al. 2009; Tian, Deng & Chan 2009; Mocák, Muller & Siess 2011; Tkachenko et al. 2014). Numerous strategies have been employed to model the properties of convective boundaries.

Here we use the simple model of exponentially decaying convective boundary mixing (CBM) initially based on hydrodynamic simulations by Freytag, Ludwig & Steffen (1996) and first introduced in stellar evolution simulations by Herwig et al. (1997) to address the observational properties of H-deficient post-AGB stars (Werner & Herwig 2006). This or similar exponential models for CBM have been adopted and investigated for many other problems, including the ^{13}C-pocket in low-mass AGB stars (Lugaro et al. 2003; Herwig, Langer & Lugaro 2003; Cristallo et al. 2009), the observed CNO enhancement of nova ejecta and their fast rise time (Denissenkov et al. 2013) and the quenching of the C flame in super-AGB stars (Denissenkov et al. 2013) and the general properties of AGB stellar models (Herwig 2000; Miller Bertolami et al. 2006; Weiss & Ferguson 2009). A quantitative determination of the CBM efficiency in terms of the e-folding distance of the diffusion coefficient by analysis of hydrodynamic simulations has been attempted by Herwig et al. (2007), but the results obtained so far are preliminary because they are based on 2D calculations.

The evolution of super-AGB stars is characterised by the ignition of C burning that will lead to the formation of an electron-degenerate ONe core (Garcia-Berro et al. 1994). The details of the outcome of C burning has been shown to depend on the assumptions for convective boundaries. Denissenkov et al. (2013), Chen et al. (2014) and Farmer, Fields & Timmes (2015) have demonstrated that in models in which convective boundary mixing is taken into account the C-flame is quenched and hybrid CONe WDs may form, with numerous possible consequences that impact, for example, upon the progenitor evolution of type Ia supernovae (Denissenkov et al. 2015; Kromer et al. 2015).

Further burning stages beyond C burning (i.e. Ne, O, Si) are prevented by a combination of electron degeneracy and neutrino cooling. Super-AGB stars may end their lives as ONe (or hybrid CONe; Denissenkov et al. 2013) white dwarfs or as electron-capture core collapse supernovae (Nomoto 1984, 1987; Poelarends et al. 2008; Jones et al. 2013; Doherty et al. 2015). The evolution up to the thermally pulsing super-AGB phase is characterized by several dredge-up (DUP) events, including, in some cases, a dredge-out event that brings larger amounts of He-burning products to the surface (e.g. Ritossa, García-Berro & Iben 1999; Siess 2007; Herwig et al. 2012). Since the evolution of the H-shell depends on the abundance of (C+N+O), super-AGB thermal pulse stars that have enhanced C and O abundances because of this dredge-out will afterwards behave as if they had larger initial C+N+O abundances.

The initial mass range for entering the super-AGB phase is rather narrow, from $\approx 7.5 - 9.25\ M_\odot$ at solar metallicity according to Poelarends et al. (2008), $8 - 9.75\ M_\odot$ according to Doherty et al. (2015) and $7 - 9\ M_\odot$ according to Woosley & Heger (2015). This result is uncertain as it depends sensitively on the treatment of the H- and the He-core convection boundary. The exact mass range will also depend on the uncertain ^{12}C + ^{12}C nuclear reaction rate. The limiting initial mass for C ignition decreases from about $7.1\ M_\odot$ to about $5.4\ M_\odot$ when the C-burning rate is increased from $0.1\lambda_{\rm CF88}$ to $1000\lambda_{\rm CF88}$ (Chen et al. 2014), where $\lambda_{\rm CF88}$ is the rate from Caughlan & Fowler (1988). This corresponds to a decrease in the limiting core mass from $1.1\ M_\odot$ to $0.93\ M_\odot$. At lower metallicity the mass range for the formation of super-AGB stars will span lower initial masses (see, e.g., Siess 2007).

The composition of the wind ejecta and evolutionary fate of super-AGB stars at low metallicity is of particular importance for the interpretation of multiple populations observed in some globular clusters, in particular the He-rich blue main-sequence in Ω Cen (Anderson 1997) and several other clusters. These second (or third) generation populations have also unusual C, N and O abundances and models of super-AGB stars (e.g. Ventura & D'Antona 2011; Herwig et al. 2012; Karakas, Marino & Nataf 2014) have been used to address the abundance anomalies of distinct populations in globular clusters. Herwig et al. (2012) have proposed the *Galactic plane passage gas purging chemical evolution scenario* to integrate photometric and stellar evolution information with dynamic constraints from the cluster's orbit to address many of the observed abundance properties of the distinct populations in Ω Cen. In this work we are reporting on further, and more detailed investigations of the super-AGB phase in stellar models.

Different groups using different stellar evolution codes obtain reasonably similar results for the super-AGB evolution if the same assumptions (in particular for mixing) are made (Poelarends et al. 2008; Siess 2010; Doherty et al. 2010, 2014). While some of these studies go beyond the strict Schwarzschild criterion for convection, none of these previous investigations have, to our knowledge, explored the effect of variable CBM efficiencies.

The effect of CBM in low-mass AGB stars has been investigated in detail via simple CBM algorithms which effectively model a mixing diffusion coefficient that exponentially decreases with geometric distance from the convection boundary (Herwig et al. 1997; Mazzitelli, D'Antona & Ventura 1999; Herwig 2000; Miller Bertolami et al. 2006; Weiss & Ferguson 2009). The consequences of CBM for He-shell flash convection are larger ^{12}C and ^{16}O abundances in the intershell, in agreement with observations of H-deficient post-AGB stars (Werner & Herwig 2006), and larger peak temperatures for the ^{22}Ne-fuelled *s*-process contribution. Lugaro et al. (2003) have argued that this may lead to isotopic ratio predictions, for example for Zr, that could be incompatible with observations from pre-solar grains. This question needs to be revisited however, considering possible modifications to the details of the mixing algorithm as well as the latest nuclear reaction rate data, in particular for the ^{22}Ne$(\alpha, n)^{25}$Mg neutron source reaction rate (e.g. Longland, Iliadis & Karakas 2012; Bisterzo et al. 2015) and Zr neutron capture rates (Lugaro et al. 2014; Liu et al. 2014). Denissenkov et al. (2013) have shown that with exponential-diffusive CBM the observed enhancement of C and O in nova ejecta and the fast rise time of the nova light curve can be reproduced in 1D models. CBM has been reported in multidimensional simulations of nova shell flashes (Casanova et al. 2011; Glasner, Livne & Truran 2012). It is also accepted that CBM in the form of some sort of overshooting prescription needs to be employed during the core H-burning phase on the main sequence, and almost all stellar evolution calculations do account for this convection-induced extra mixing.

Rotationally-induced mixing at the bottom of the convection zone has been shown to be insufficient in spherically-symmetric simulations (Herwig 2003b; Siess, Goriely & Langer 2004) to model the partial mixing between the H-rich envelope and the ^{12}C-rich core that leads to the formation of the ^{13}C-pocket in low-mass AGB stars (e.g. Herwig 2000; Cristallo et al. 2009). In addition, it may reduce significantly the *s*-process yields (Piersanti, Cristallo & Straniero 2013). How well rotationally-induced mixing can be approximated in one-dimensional models of stars is unclear at present.

Thus, there is significant motivation to investigate how the evolution of super-AGB stars proceeds if small and moderate efficiencies of CBM are taken into account at all convective boundaries. In the case of super-AGB stars, this makes the computa-

tions numerically much more demanding, and in many cases the quantitative details of the results have to be considered as very uncertain. This is so because (i) the exact amount and efficiency of CBM is presently unknown for the convection boundaries in super-AGB stars, and (ii) we frequently encounter in these calculations of convective-reactive H-combustion regimes that at least locally violate some of the assumptions that are the basis of 1D spherically symmetric stellar evolution codes with the mixing-length theory for convection. In that sense, the computations presented here are in a way to be considered as a road map which points out areas in which more detailed 3D hydrodynamic investigations need to be performed in the future.

In this paper we report on the occurrence of convective-reactive H-combustion flashes in super-AGB thermal pulses in stellar models when CBM is included. These H-ingestion flashes present specific differences from H-ingestion flashes found previously in normal AGB stars of very low metallicity (e.g. Fujimoto, Ikeda & Iben 2000; Herwig 2003a; Suda et al. 2004; Campbell & Lattanzio 2008; Cristallo et al. 2009). In particular, the latter are usually a one-off event which removes, through copious dredge-up of C and O, the conditions for its occurrence. The H-combustion flashes we observe in super-AGB stars can be recurrent as they are initiated after the peak He-burning luminosity of each shell flash as a result of a very fast and efficient dredge-up while the He-shell is still convective. Nevertheless, the nucleosynthesis processes following the ingestion are expected to be quite similar, being driven by a fast burning of protons and by the consequent formation of ^{13}C.

The ^{13}C made by H-^{12}C combustion activates the ^{13}C$(\alpha,n)^{16}$O reaction, producing an intermediate neutron density of $N_{\rm n} \approx 10^{15}$cm^{-3}, defined as the *i* process by Cowan & Rose (1977). We adopt this designation for all n-capture regimes driven by convective burning of protons in He-burning convection zones. Such conditions can be found in numerous stellar environments, particularly in stars of very low metallicity, such as the the He-core flash in low-metallicity stars (Campbell, Lugaro & Karakas 2010).

As shown recently by Herwig et al. (2011) 1D stellar evolution simulations with mixing-length theory for convection do not predict surface observed abundances of the post-AGB H-ingestion star Sakurai's object. Instead, alternate mixing assumptions had to be made for that reactive-convective event, based on its hydrodynamic nature. Recent attempts of hydrodynamic simulations of the H-ingestion event in Sakurai's object have shown a much more violent behaviour than expected from stellar evolution models, and led to the discovery of the global oscillation of shell-H ingestion (GOSH; Herwig et al. 2014). The GOSH is a non-radial instability that develops out of a spherically symmetric initial state, and rearranges the internal stratification in ways that would have been impossible to predict based on stellar evolution simulations alone. The GOSH simulations of Herwig et al. (2014) only cover a first non-radial instability which is likely to be followed by further violent and non-radial hydrodynamic events. Validated sub-grid models for reactive-convective regions to be employed in stellar evolution models are therefore not yet available, and thus we have to consider stellar evolution results as uncertain once the convective-reactive phases are occurring.

With these caveats in mind we will briefly present the physics assumptions for our simulations in Section 2. In Section 3 we describe the main results. In Sections 4 and 5 we discuss the potential consequences of our results.

2 METHOD

2.1 Stellar evolution code and physics assumptions

For the stellar evolution simulations presented here we use the MESA code (Paxton et al. 2011, 2013, 2015)[1]. The MESA papers by Paxton et al. already contain verification cases for a wide range of stellar evolution scenarios, including thermal pulses and dredge-up in AGB stars. In addition, we have now also run massive AGB models with the same initial abundances and similar enough physics assumptions as those chosen for the grid of models including massive AGB stars by Herwig (2004b) obtained with the EVOL stellar evolution code, and we find the MESA results again to be in good agreement.

We use a custom nuclear network with 31 species—based on the MESA network `agb.net`—including the major isotopes for elements from H to Al and closing with ^{28}Si. For reactions we included PP-chains, CNO cycles, the NeNa and MgAl cycles, $3\alpha \rightarrow {}^{12}$C, ^{12}C$(\alpha,\gamma)^{16}$O, ^{13}C$(\alpha,n)^{16}$O, and ^{12}C + ^{12}C (both α and p exit channels), amongst other less critical reactions. Although we included the ^{13}N isotope explicitly we did not include the ^{13}N$(p,\gamma)^{14}$O reaction, which would have been relevant. However, this omission will not change any of the main findings, and will be corrected along with several other approximations to the network in a forthcoming more detailed nucleosynthesis investigation of these models. Reaction rates are taken from the NACRE compilation (Angulo, Arnould & Rayet, M. et al. 1999).

The mixing length theory of convection (MLT) is employed to calculate the temperature gradient in the convective regions and predict the convective velocities. Mixing in convective regions is approximated as a diffusive process with diffusion coefficient $D = \frac{1}{3} v \alpha_{\rm MLT} H_P$, where v is the convective velocity according to MLT and H_P the scale height of pressure. For the mixing-length parameter we adopt $\alpha_{\rm MLT} = 1.73$. In addition to the default mesh controls we refine the mesh on the abundances of H, ^{4}He, ^{13}C and ^{14}N. Additional criteria are added to resolve He-shell flashes and the advance in time of the thin H-burning shell during the interpulse phase. We use the atmosphere option `'simple_photosphere'`, which gives the surface pressure as

$$P_s = \frac{2GM}{3\kappa_s R^2}\left[1 + 1.6\times10^{-4}\kappa_s\left(\frac{L/L_\odot}{M/M_\odot}\right)\right] \quad (1)$$

(see Paxton et al. 2011 and Cox & Giuli 1968, Section 20.1). κ_s is the surface opacity, for which an initial guess is made and converged iteratively with the pressure. We assume a mass loss rate of $\log(\dot{M}/\,M_\odot\,{\rm yr}^{-1}) \approx -4.8$ which is obtained by using the the Blöcker (1995) mass loss rate in MESA with $\eta = 5\times10^{-4}$. This is likely to be at the low end of a rather uncertain range of possible mass loss rates for these stars. We adopt the OPAL C- and O-enhanced opacities in MESA (Iglesias & Rogers 1996).

2.2 Convective boundary mixing

We have discussed convective boundary mixing (CBM) and some evidence from hydrodynamic simulations in the Introduction. Note that we are avoiding the term overshooting and instead prefer to describe a wide range of hydrodynamic instabilities that can be observed at and near convective boundaries as CBM. A variety of

[1] details about the versions of the MESA code that were used will be made available online along with the inlists.

fluid dynamics processes and hydrodynamic instabilities can contribute to CBM, such as buoyancy-driven overshooting of coherent convective systems (Freytag, Ludwig & Steffen 1996), Kelvin-Helmholtz instabilities (Meakin & Arnett 2007; Casanova et al. 2011) which in turn may be enabled by boundary-layer separation (Woodward, Herwig & Lin 2015), or mixing due to internal gravity waves (Denissenkov & Tout 2003).

As we described in the Introduction, our stellar evolution simulations approximate abundance mixing due to these CBM processes—no matter what their physical origin is—via the exponentially decaying mixing algorithm described in Freytag, Ludwig & Steffen (1996) and first applied in stellar evolution calculations by Herwig et al. (1997). In this approximation, the diffusion coefficient takes the form

$$D_{\rm CBM} = D_0 \exp\left(-\frac{2|r-r_0|}{fH_P}\right), \quad (2)$$

where H_P is the pressure scale height and D_0 is the diffusion coefficient given by the mixing length theory of convection at a location r_0. f is a parameter defining the e-folding length fH_P of the diffusion coefficient.

D_0 is not defined at the convective boundary because in MLT, the convective velocity is zero there. Instead of taking D_0 at the last convective zone, the MESA implementation allows to specify how far inside the convection zone from the boundary the exponential decay should begin. The Eulerian coordinate of this location is then r_0. Indeed, the results of Freytag, Ludwig & Steffen (1996, their Figs. 10 and 14) and Herwig et al. (2006, their Fig. 24) show that the decay of the radial component of the convective velocity and of the inferred radial diffusion coefficient begins inside the convective zone and not at the formal convective boundary. In the MESA implementation, there is a second parameter for each convective boundary f_0, which specifies how far from the convective boundary, on the convective side, the decay should begin. This distance is $f_0 H_P$. In our models, we use $f_0 = f$ at all convective boundaries. The diffusion coefficient as formulated in Eq. 2 is then applied in the direction of the convective boundary and across into the stable layer.

The value of f has no direct, simple and intuitive relation to the physical flow properties—other than larger values indicate more efficient and more spatially extended mixing than smaller values—because it is a number that, when multiplied by the local scale height of pressure, gives the e-folding length of the diffusion coefficient that is representing mostly non-diffusive mixing processes caused by a variety of hydrodynamic processes.

For our benchmark model we have assumed $f = 0.014$ at all convective boundaries (including the H- and He-core burning phases), except at the bottom of the convective envelope (including during the third dredge-up, TDU, if it occurs) where we assume $f_{\rm env} = 0.0035$, and at the bottom of the pulse-driven convection zone (PDCZ) where we assume $f_{\rm PDCZ} = 0.002$. The values of $f_{\rm env}$ and $f_{\rm PDCZ}$ are lower by a factor of about 36 and 4 respectively compared to what we usually assume in our low-mass AGB simulations (which generally agree with observations in post-AGB H-deficient stars and planetary nebulae; e.g. Werner & Herwig 2006; Pignatari et al. 2013; Delgado-Inglada et al. 2015) and compared to what has been shown to reproduce observational characteristics of nova shell flashes (Denissenkov et al. 2013). As discussed previously by Herwig (2004) and Goriely & Siess (2004), dredge-up may be *hot* in (super-) AGB stars of low metallicity and larger initial mass, where the H-burning at the bottom of the convective envelope can become important already during the dredge-up phase. Another way to look at it is that the familiar hot-bottom burning already starts during the third dredge-up in AGB stars of low metallicity and larger initial mass. As discussed briefly by Herwig (2004), a larger CBM efficiency during the dredge-up phase in massive AGB or super-AGB stars may result in the formation of a corrosive H-burning flame that may terminate the AGB through enhanced mass loss.

When hydrogen is burning at the bottom of the convective envelope, the boundary will be stiffer (lower CBM efficiency) because of the entropy barrier produced in the vicinity of the burning shell. Unfortunately, without detailed hydrodynamics simulations or fluid experiments, it is difficult to know how much stiffer the boundary becomes. In addition, translating such a stiffness into a CBM parameter $f_{\rm env}$ is not straightforward. The choice of $f_{\rm PDCZ} = 0.008$ below shell-flash convection zones on top of degenerate cores is a good starting point, with a similar value being able to reproduce the intershell abundances of post-AGB stars and the ejecta enrichment and fast light curve rise times of novae (Werner & Herwig 2006; Denissenkov et al. 2013). However, the conditions in the shell flashes of super-AGB stars, post-AGB stars and novae are certainly not identical. For example, in post-AGB stars the peak luminosities are higher than those in super-AGB stars by roughly an order of magnitude. Furthermore, the stiffness of the convective boundaries and the aspect ratio of the convection will naturally also vary from site to site. The correlation of CBM efficiency with nuclear energy generation rate or driving luminosity of the convection is no easy task and requires detailed, targeted study. For these reasons we study a range of values for $f_{\rm env}$ and $f_{\rm PDCZ}$ in the present work with a view to motivating such targeted studies.

Again, the details will depend critically on the assumed mixing properties at the convective boundaries which need to be investigated eventually by means of three-dimensional stellar hydrodynamics simulations. We address this uncertainty by providing a parameter study of the dependence of our H-ingestion results on the CBM parameters. As we will describe in Section 3, H-ingestion in our TP-SAGB models is highly sensitive to CBM at the base of the PDCZ and at the base of the hot-bottom-burning H-envelope during TDU. These affect the response time or rate of the dredge-up as well as its depth (see Mowlavi 1999; Herwig 2004a). The CBM *above* the PDCZ, which is a critical factor in the H-ingestion He-shell flashes of low-metallicity AGB stars and VLTPs in post-AGB stars, is of less importance here. Indeed, we have computed models with a range of CBM efficiencies above the PDCZ and it is clear that this CBM does not initiate a H-ingestion TP in our TP-SAGB models unless unjustifiably high efficiencies are used. The overshoot at the top of the PDCZ has been studied by Herwig, Blöcker & Driebe (2000), who also find no significant impact of this CBM on the proximity of the PDCZ to the convective H envelope. Thus, we limit our parameter study to only $f_{\rm env}$ and $f_{\rm PDCZ}$.

3 STELLAR EVOLUTION MODELS

The evolution up to the beginning of the thermal pulse phase proceeds in a similar manner to that described in previous studies (e.g. Ritossa, García-Berro & Iben 1999; Siess 2007; Doherty et al. 2010; Ventura & D'Antona 2011; Jones et al. 2013). The abundance signature of the early AGB during the second dredge-up is a significant enhancement of He to a mass fraction of about 0.37. This is followed in the more massive super-AGB models by a 'dredge-out' after the carbon shell burning episodes, which can be considered as another dredge-up event following an initial convective He-shell burning episode that precedes the regular thermal pulses. This mix-

ing event brings large amounts of C and O to the surface (see, e.g., Ritossa, García-Berro & Iben 1999; Siess 2007; Herwig et al. 2012, and Section 3.1).

Afterwards, the bottom of the convective envelope continues to corrosively penetrate further into the He-burning ashes and the H-free core is reduced by an additional $\Delta m_{\rm r} \approx 10^{-2}\,M_{\odot}$. This last dredge-up phase before the onset of regular thermal pulses is facilitated by CBM. As described in Herwig (2004), H is mixed into a very thin layer below the Schwarzschild convective boundary and generates there H-burning luminosities of the order $\log L_{\rm H}/L_{\odot} \approx 5.5$. This mixing-induced H-flame will continue until the conditions for dredge-up are removed, i.e. the excess energy from previous nuclear flashes and core contraction has escaped the envelope. However, in view of preceding and following mixing and burning events, this short phase of H-flame core penetration does not have a large effect, except that the transformation of C and O into ^{14}N is starting during this phase, but only getting fully underway during the following thermal pulse phase.

3.1 H-^{12}C combustion during dredge-out

The most massive super-AGB stars and failed massive stars (Jones et al. 2013) experience a dredge-out event (Ritossa, García-Berro & Iben 1999; Siess 2007; Doherty et al. 2015). This is when shell helium burning releases enough energy to induce convection during the second DUP, as mentioned briefly above. A combination of the release of gravo-thermal energy and of nuclear energy cause the helium-shell convection zone to grow (outwards) in mass and merge with the descending base of the convective hydrogen envelope (Fig. 1). There are three main reactions contributing to the nuclear energy generation during this phase: ^{12}C + ^{12}C, ^{12}C$(\alpha,\gamma)^{16}$O and the triple-α reaction. The energy sources are physically stratified in only a very thin (roughly $3\times10^{-2}\,M_{\odot}$) mass shell (see Fig. 2).

The two main consequences of dredge-out are the enrichment of the envelope with ashes of hydrogen burning and incomplete He burning, and the advection of protons down to He-burning temperatures where primary ^{12}C is present with a typical mass fraction of $X(^{12}\mathrm{C}) \approx 0.5$. A strong flash occurs as the protons are mixed rapidly into the hotter layers below the base of the H envelope. This has previously been reported by Gil-Pons & Doherty (2010), who found that the resulting hydrogen burning produced local luminosities in excess of 10^6 L$_{\odot}$. As we will describe here our models suggest that in rapid combustion of the H with ^{12}C local luminosities well in excess of 10^9 L$_{\odot}$ may be reached.

The dredge-out event is illustrated in Fig. 1 for a 7.5 $M_{\odot}$ $Z = 10^{-3}$ model (top panel) and for a 8.4 $M_{\odot}$ $Z = 0.01$ model (bottom panel). In this simulation the strict Schwarzschild criterion (i.e. no CBM) is assumed at the lower boundary of the convective envelope. Our simulations confirm that dredge-out is encountered without CBM at the lower boundary of the convective envelope. Dredge-out has been reported and described also by, e.g., Ritossa, García-Berro & Iben (1999), Siess (2007), Gil-Pons & Doherty (2010) and Doherty et al. (2015), none of whom prescribe for CBM (though each group has their own method of treating the convective boundary). We have simulated massive super-AGB and failed massive stars with initial metallicities between $Z = 10^{-5}$ and 0.02, and dredge-out is seen to occur at all metallicities when holding our CBM assumptions described in Section 2.2 *and* when setting $f_{\rm env} = 0$.

During the dredge-out, protons are mixed down through the helium shell toward higher temperatures. In the 8.4 $M_{\odot}$, $Z = 0.01$ model the protons reach temperatures in excess of 2×10^8K, where their fraction by mass is a few 10^{-6}. The energy generation at this location reaches a few 10^{13} erg g^{-1} s^{-1}. The abundance profiles, temperature stratification and specific nuclear energy generation at the time of peak nuclear energy generation are shown in Fig. 3 and these characteristics are summarised again in Table 1.

In order to characterize the dynamic importance of the convective-reactive nuclear energy release we introduce a dimensionless number which relates the nuclear energy released to the

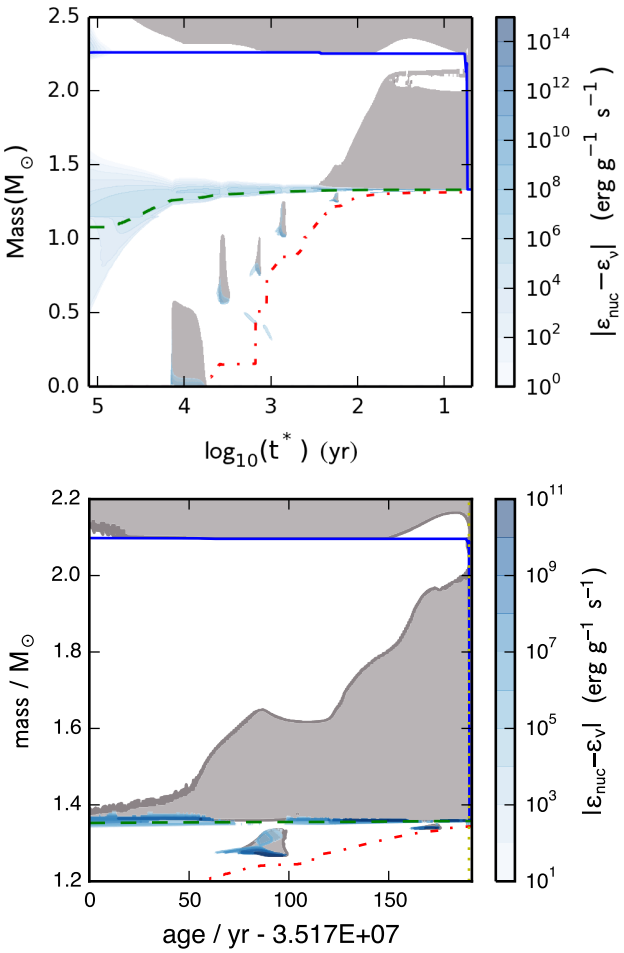


Figure 1. Top panel: evolution of the convective structure and energy generation during dredge-out in a 7.5 $M_{\odot}$ Z=0.001 stellar model. t^* is the time remaining until the end of the calculation. Grey regions are convectively unstable according to the Schwarzschild criterion while white regions are stable. The solid (blue), dashed (green) and dot-dashed (red) lines indicate the H-free, He-free and C-free core boundaries, respectively. A convective layer develops in the He shell and grows outwards in mass towards the base of the descending convective envelope. Eventually, the two coalesce and protons are mixed down to the bottom of the He-burning shell on a convective turnover time scale. Bottom panel: same as top panel but for the 8.4 $M_{\odot}$ $Z = 0.01$ model as a function of time, zoomed in.

site	T / K	ρ / g cm^{-3}	$X_{\rm H}$	$X_{\rm C}$
dredge-out	$\sim 2\times10^8$	$\sim 2\times10^2$	$\gtrsim 10^{-6}$	$\sim 10^{-2}$
TP-SAGB	$\sim 2\times10^8$	~ 60	$\sim 3\times10^{-2}$	~ 0.2

Table 1. Characteristic conditions during H-ingestion in both dredge-out and TP-SAGB sites.

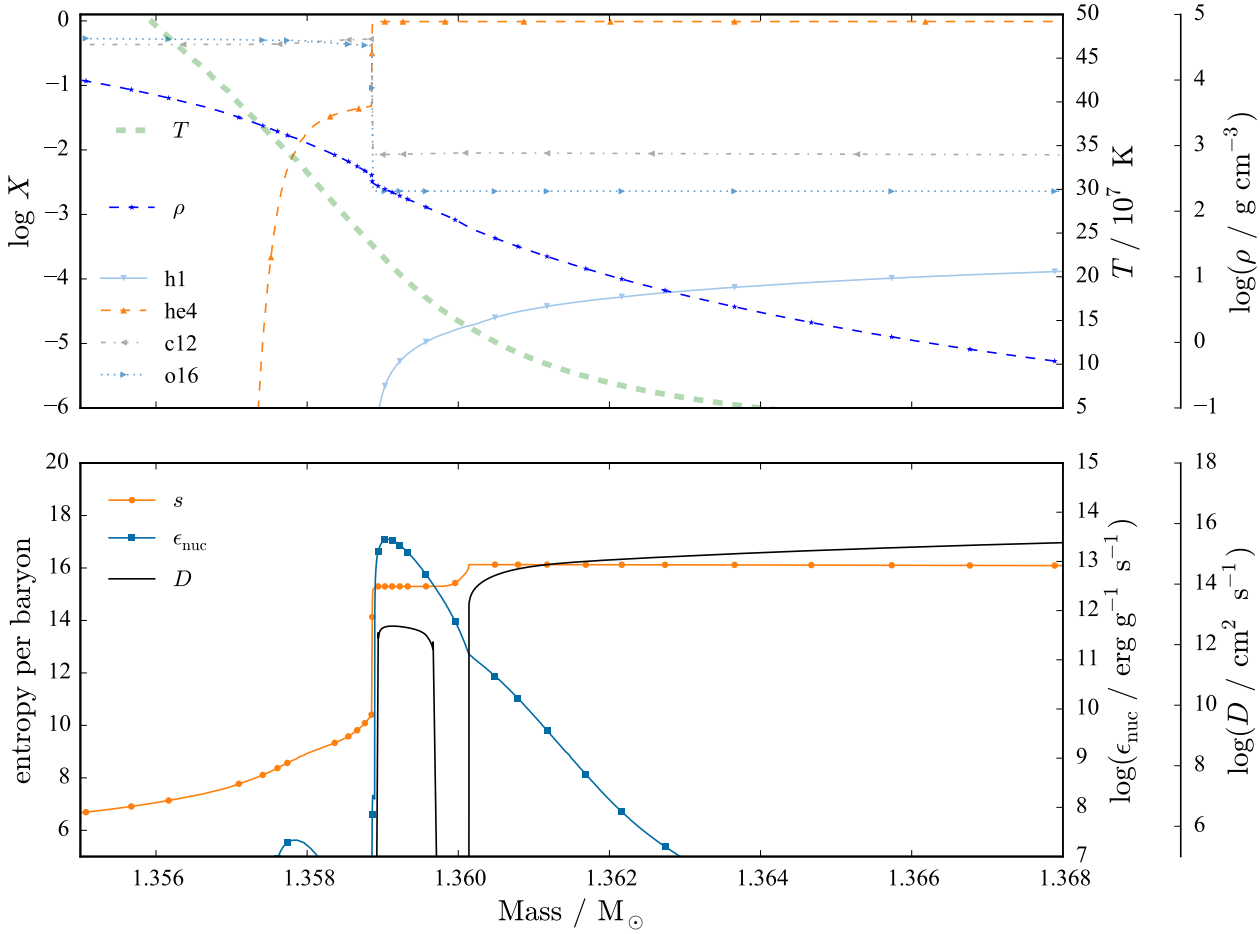


Figure 3. Abundance profiles with the temperature and density stratification (top panel), entropy s, specific energy generation rate and and diffusion coefficient (bottom panel) in the 8.4 $M_\odot$ $Z = 0.01$ model during the peak energy generation due to H-^{12}C combustion (very right hand side of Fig. 1, bottom panel, where the solid blue H-free core boundary penetrates down to the green dashed He-free core boundary, indicated by a vertical dotted yellow line). The points are illustrative and do not reflect the grid. At the base of the convective helium layer (just below mass coordinate 1.360 $M_\odot$), the mass fraction of protons is a few 10^{-6} and the temperature is in excess of 2×10^8 K. These are precisely the conditions under which the neutron densities characteristic of the i-process can be achieved due to the release of neutrons in the $^{12}\mathrm{C}(p,\gamma)^{13}\mathrm{N}(\beta^+\nu)^{13}\mathrm{C}(\alpha,n)^{16}\mathrm{O}$ reaction chain. In our 1D hydrostatic simulations the protons burn as they are transported inwards through regions of increasing temperature. The burning taking place at mass coordinate $M_r \approx 1.360\,M_\odot$ increases the entropy and causes a split in the convection zone, which can be seen as a break in the diffusion coefficient profile.

internal energy. As protons are advected into the He-shell convection they will encounter increasing temperature and primary ^{12}C with mass fraction well above 10%. A large amount of nuclear energy is released on the convective advection time scale via the $^{12}\mathrm{C}(p,\gamma)^{13}\mathrm{N}$ reaction (see appendix A.2 in Herwig et al. 2011). The fastest time scale on which this energy can escape under the assumption of hydrostatic equilibrium is the convective turn-over time. Thus, the product $\epsilon_{\rm nuc}\tau_{\rm conv}$ is here an estimate of the nuclear energy from convective-reactive H combustion that will accumlate in the combustion flame. We define

$$H = \frac{\epsilon_{\rm nuc}\tau_{\rm conv}}{E_{\rm int}}, \qquad (3)$$

where $\epsilon_{\rm nuc}$ is the specific energy generation from nuclear reactions, $\tau_{\rm conv}$ is a mixing timescale and $E_{\rm int}$ is the specific internal energy of the stellar material. For the mixing time scale, using the scale height of pressure at the base of the convective He-burning shell ($H_P \approx 1000$km) as a length scale and the *maximum* convective velocity predicted by MLT inside the helium-burning shell ($v_{\rm conv} \approx 3\mathrm{kms}^{-1}$), we find a lower limit of

$$\tau_{\rm conv} \approx \frac{H_P}{v_{\rm conv}} = 409\mathrm{s}. \qquad (4)$$

With these asumptions $H = 0.11$. This means that in the combustion flame layer the cumulative nuclear energy input is of the order of 11% of the internal energy, or 8% of the binding energy of the layer, or greater.

The H-number estimate suggests that the H-ingestion may release and add to the flow a significant fraction of the binding energy of the layer, in which case fundamental assumptions of stellar evolution, such as hydrostatic equilibrium and the applicability of MLT become inappropriate. Herwig et al. (2011) have shown that in another case of convective-reactive H-ingestion observations can not be reproduced with MLT/stellar evolution models. Sakurai's object is a very-late thermal pulse object with a 2-dex enhancement of first-peak n-capture elements. Only by adopting significant modifi-

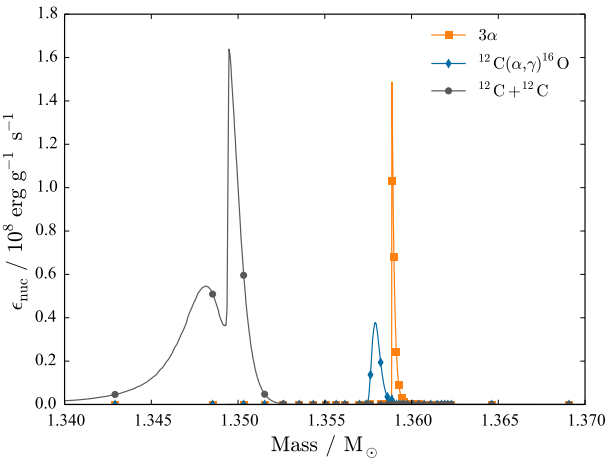


Figure 2. Stratification of the three predominant energy-generating nuclear reactions during the dredge-out phase in the 8.4 $M_\odot$ $Z = 0.01$ model from Fig. 1 (bottom panel) at a time from the right hand side of the plot where the yellow dotted line is drawn.

Z	$M_{\rm ini}$ / $M_\odot$	$M_{\rm C}^{\rm SAGB}$	H ing?	peak $L_{\rm H}$ / $10^9 L_\odot$
0.02	8.2	1.26975	N	-
0.01	8.15	1.28025	N	-
10^{-3}	7.0	1.24606	Y	8.25
10^{-4}	7.0	1.26263	Y	8.26
10^{-5}	7.2	1.27432	Y	8.48

Table 2. Summary of the models presented here as a metallicity study. These models assume $f_{\rm env} = 0.0035$ and $f_{\rm PDCZ} = 0.002$ (see text for details). $M_{\rm C}^{\rm SAGB}$ is the mass of the H-free core at the first thermal pulse. Also given is whether or not a H-ingestion TP is encountered and if so, the peak H-burning luminosity is given.

cations to the MLT mixing predictions could nucleosynthesis simulations reproduce the observations. Herwig et al. (2014) presented hydrodynamic simulations of the H-ingestion event in Sakurai's object and reported a non-radial global oscillation of shell H-ingestion (GOSH) for a situation similar to the one encountered here for the H-ingestion during the dredge-out. We therefore conclude in a similar manner that these stellar evolution models with MLT, and estimates such as as the *H*-number based on these models, are not entirely realistic once the H-ingestion event with a large *H*-number occurs.

The peak energy generation due to H-^{12}C combustion during the dredge-out is short-lived in our MLT stellar evolution models. The burning of protons as they are transported inwards modifies the entropy structure of the region of interest. The entropy and diffusion coefficient profiles are shown in Fig. 3. In the stellar evolution model the entropy produced by the burning of hydrogen causes a split in the convection zone, resulting in two convective regions that do not mix further. The protons in the lower convective zone are quickly destroyed, after which fresh hydrogen brought down is burned at the top of the split. There, the temperature is only $\approx 1.5 \times 10^8$ K but nevertheless a few 10^{-3} in mass fraction of ^{13}C is produced. A split in the diffusion coefficient under similar conditions was seen in the models of Herwig et al. (2011). The authors found that the basic assumptions that contribute to the formation of the split—such as a spherically symmetric H-abundance and a spherically symmetric inward diffusion of H—were not found in three-dimensional hydrodynamic simulations. Hence the hypothesis that two convective regions should mix to some extent.

This modified mixing assumption by Herwig et al. (2011) (whereby the two convection zones split by the formation of the entropy barrier due to H-burning are allowed to continue to mix) leads to n-capture nucleosynthesis at neutron densities of $N_{\rm n} \approx 10^{15}$cm^{-3}. This is approximately two orders of magnitude higher than in the highest neutron densities encountered in the *s*-process powered by the ^{22}Ne neutron source in the He-shell flash convection zone of massive AGB stars (see, e.g., Straniero, Cristallo & Piersanti 2014, their Table 1). This n-capture regime has been labelled the intermediate regime, or *i*-process by Cowan & Rose (1977). We propose that the H-ingestion induced hydrodynamics in the super-AGB dredge-out He-burning convection zone would behave similarly to the situation investigated for the H-ingestion event in Sakurai's object, in the sense that further mixing between the convecion zones will lead in a similar way to the copious production of ^{13}C and the associated intense neutron burst (see, e.g., Lugaro, Campbell & de Mink 2009; Campbell, Lugaro & Karakas 2010). This hypothesis will need to be tested by appropriate hydrodynamic simulations. In the meantime, based on the evidence available at this time we adopt as the most likely scenario that the dredge-out in super-AGB stars is a site for *i*-process nucleosynthesis (see §4).

In failed massive stars that would become electron-capture supernovae, the dredge-out occurs about 30 years before the explosion. With hydrodynamics simulations suggesting that the flow of protons into the He-burning layer should persist it is entirely possible that enough energy is released in the ingestion to unbind and eject material that has been exposed to such large energy generation rates. Without detailed multi-physics simulations it is very difficult to know to what extent energy is dissipated during the ingestion/ejection event, but nevertheless we entertain this possibility and examine it in more detail in §4.2, where we also predict what the light curve of such a transient might look like.

3.2 TP-SAGB models and thermal pulse evolution

We have calculated TP-SAGB models with initial metallicities of $Z = 0.02$, 0.01, 10^{-3}, 10^{-4} and 10^{-5} (Table 2). These models were computed holding the input physics assumptions described in Section 2.2. The thermal pulse properties are sensitive to the core mass, and therefore the initial masses were chosen such that the CO core masses of all the models at the first thermal pulse were similar (the standard deviation in the CO core masses at the first thermal pulse is 0.012 $M_\odot$; see Table 2).

The purpose of this metallicity survey in the models is to compare the thermal pulse properties of the super-AGB models at different metallicities with regards to approaching the conditions for a H-ingestion event to take place. H-ingestion occurs in our TP-SAGB models, as we will show, when the third dredge-up (TDU; the deepening of the convective envelope in mass following the thermal pulse; see Fig. 4), facilitated by CBM, reaches into the pulse-driven convection zone (PDCZ). In order for this to happen, the TDU must be rapid enough, and deep enough, to cause a convective exchange of material between the convective H-envelope and the PDCZ.

A TDU event regularly follows each He-shell flash although is often absent for the first few flashes. As the models evolve along the TP-SAGB, the time Δt between the extinction of the PDCZ t_1

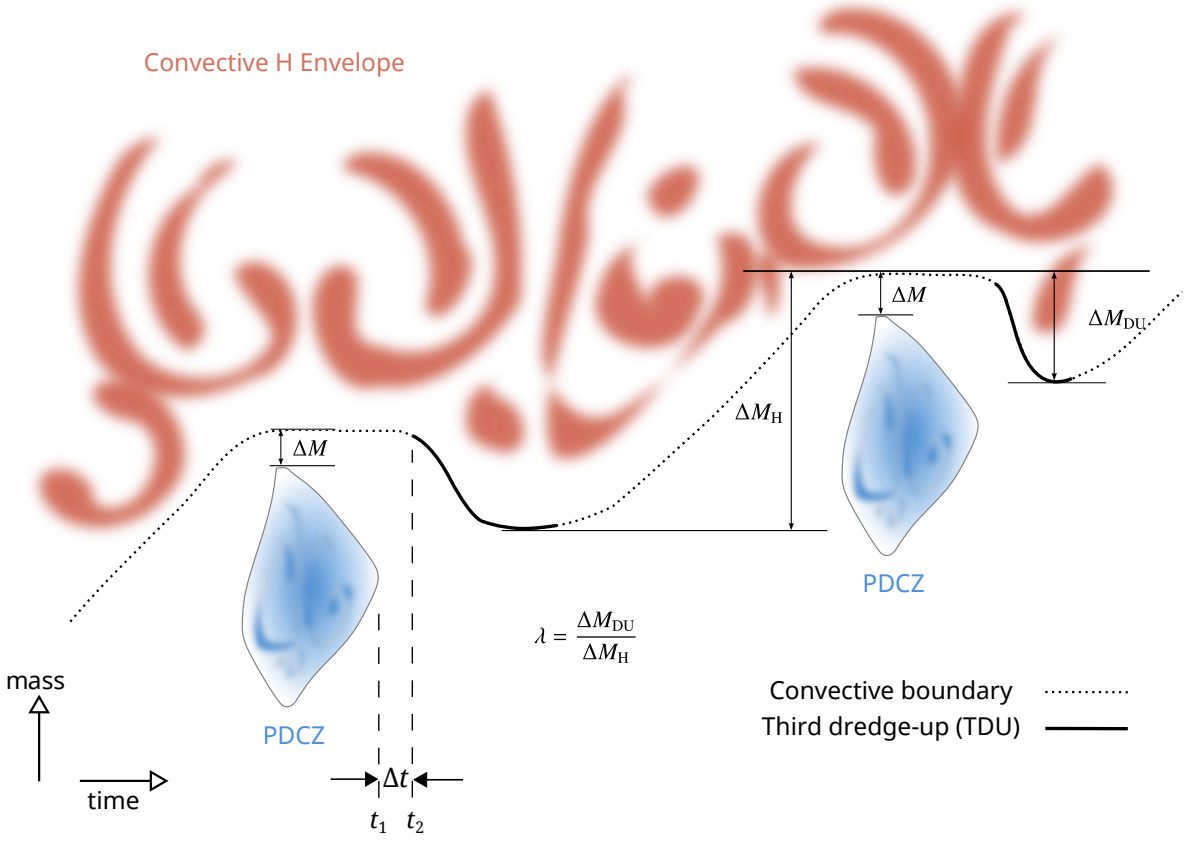


Figure 4. Illustration of the TP-SAGB phase, defining the pulse-driven convection zone (PDCZ), the convective envelope base penetration (CEBP), t_1 and t_2 – the times of PDCZ extinction and beginning of CEBP, respectively – and the time interval between t_1 and t_2, Δt.

and the beginning of the TDU t_2 becomes shorter (see definitions in the illustration in Fig. 4). This trend is seen for models at all metallicities that we have considered and is shown in Fig. 5 (top panel; see also Mowlavi 1999 and Herwig 2000). We define the beginning of the TDU in these models as the time when the base of the convective envelope has deepened in mass by 1% of $\Delta M_{\rm DU}$ for a given TDU. Of particular note is the result that after about 10–15 pulses (depending on the initial metallicity) the TDU starts while the PDCZ is still active, with the lower metallicity models reaching this point earlier in the TP-SAGB. In this case $\Delta t < 0$ (Fig. 5, top panel), which is one of the criteria for hydrogen from the envelope to be ingested into the PDCZ. If Δt were always positive then the kind of ingestion that we describe here, where the hot TDU reaches the PDCZ, could never happen. Even if we do not always see explicitly the H-ingestion in 1D models, one of the main conditions for this to happen—i.e. the TDU beginning already at the time when the PDCZ is still active—is given robustly after at most 16 thermal pulses at all initial metallicities for which we have computed models (Table 2 and Fig. 5, top panel).

The TDU efficiency λ is defined as the ratio of dredged-up mass $\Delta M_{\rm DU}$ to core-growth $\Delta M_{\rm H}$ since the end of the previous TDU (see, e.g., Lugaro et al. 2003, and Fig. 4). In our models TDU is not always deep enough to mix He-burning products to the surface (i.e. $\Delta M_{\rm DU}$ is not always larger than ΔM). For $\Delta M_{\rm DU} < \Delta M$, neither does the model experience a H-ingestion thermal pulse.

λ is consistently higher for the models with $Z \leqslant 10^{-3}$ than higher-Z models for a similar pulse number. In fact, the models with $Z \leqslant 10^{-3}$ all experience efficient TDUs from the fifteenth thermal pulse at the latest, with $\lambda > 0.5$. Indeed, in this set of models with $f_{\rm env} = 0.0035$ and $f_{\rm PDCZ} = 0.002$ we find that the models with $Z \leqslant 10^{-3}$ experience H-ingestion TPs with peak H-burning luminosities reaching almost 10^{10} $L_\odot$ (Table 2). The $Z = 0.02$ and 0.01 models also show marked increases in λ further along the TP-SAGB but in our simulations up to the 26th and 25th thermal pulses, respectively, $\lambda < 0.5$ and no H-ingestion events were encountered. An important implication of large λ values in super-AGB stars is the narrowing (or disappearance) of the electron-capture supernova channel due to a suppressed core growth rate.

The CBM parameter $f_{\rm env}$ (see §2.2) can be calibrated for the lower envelope convection boundaries during the TDU for low-mass AGB stars to reproduce the required partial mixing between the H-rich envelope and the ^{12}C-rich core to form a sufficiently large ^{13}C-pocket for the *s*-process. Lugaro et al. (2003) have proposed that a CBM parameter $f_{\rm env} = 0.128$ would reproduce *s*-process-observables. However, Pignatari et al. (2013) have shown that with $f_{\rm env} = 0.126$ the galactic C-rich stars with the high-

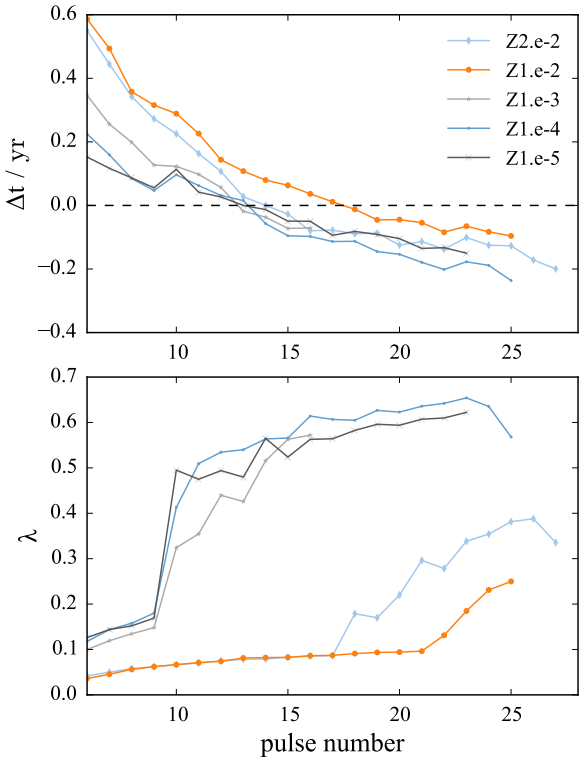


Figure 5. *Top Panel:* Time between the extinction of the pulse-driven convection zone (PDCZ) and the beginning of third dredge-up (TDU), Δt (see Fig 4 and the text for details). Hence, above the horizontal dashed line at $\Delta t = 0$ the TDU begins after the extinction of the PDCZ and below the line $\Delta t = 0$ the TDU begins while the PDCZ is still active. *Bottom panel:* TDU efficiency λ—the ratio of the mass of material mixed up to the amount the H-free core grew during the preceding H-burning inter-pulse phase—as a function of pulse number for different metallicity models.

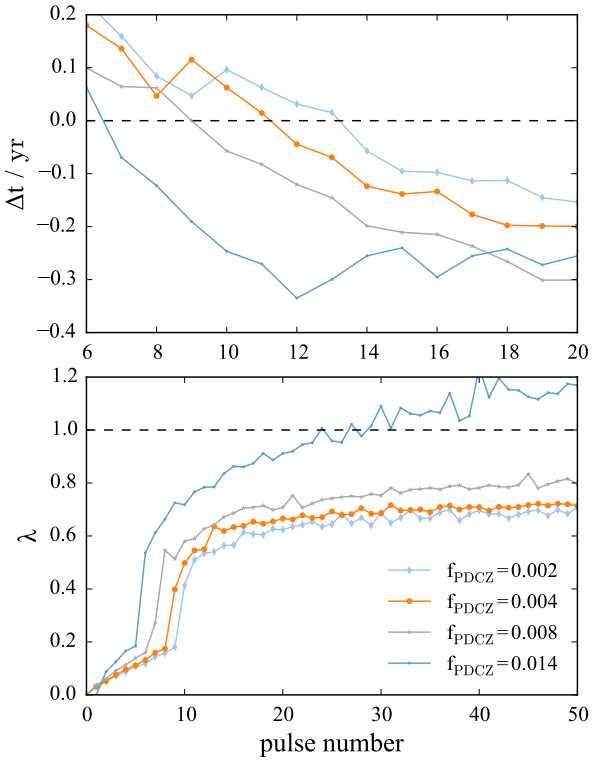


Figure 6. A series of models with $M = 7\ M_\odot$ and $Z = 10^{-4}$ in which $f_{\rm env} = 0.0035$ and $f_{\rm PDCZ}$ is increased from 0.002 through 0.014 (first 4 entries in Table 3). *Top panel*: same as Fig. 5 (top panel). *Bottom panel*: same as Fig. 5 (bottom panel).

est s-process enrichments are not reproduced (see e.g., Abia et al. 2002 and Zamora et al. 2009 for observations). The CBM at the bottom of the convective envelope during the TDU in high-mass AGB and super-AGB stars leads to hot dredge-up (see §2.2). The appropriate value for $f_{\rm env}$ is not known for this situation, but numerical experiments show that adopting the same value that was calibrated to satisfy the constraints of a sufficiently sized ^{13}C-pocket in low-mass stars would lead to very intense H-burning that would lead to rapid disintegration of the AGB star (Herwig 2004b). In our benchmark model we used a much smaller value of $f_{\rm env} = 0.0035$. Generally speaking, a much smaller value for hot DUP compared to regular TDU is justified because the energy released by burning protons mixed into the hot core will add buoyancy to the fluid elements which in turn will reduce the efficiency of the CBM process. While the efficiency of third dredge-up depends only very weakly on $f_{\rm env}$ in low-mass AGB stars (Mowlavi 1999) this is entirely different when the dredge-up is hot. In this case the dredge-up efficiency is strongly dependent on $f_{\rm env}$, as we will show in the following sections (see Fig. 8). The hot DUP, particularly with CBM, is a difficult phenomenon to simulate. Although it is approximated in our 1D code, the coupled behaviours of the burning and mixing together with the structural readjustment of the star following the peak He-shell flash luminosity is itself something that warrants further in-depth investigation (see also Herwig 2004a).

3.3 Impact of convective boundary mixing on the TP-SAGB phase and hydrogen-ingestion TPs

The efficiency and extent of convective boundary mixing during the TP-SAGB is not known at present. There are little to no observational diagnostics that really help to constrain such mixing. It is thus important to study the impact of the choice of the e-folding lengths of the exponentially decaying diffusion coefficient (fH_P in our CBM scheme) on the occurrence and behaviour of hydrogen ingestion events during the TP-SAGB. In order to accomplish this, we have computed a series of models from the end of the second dredge-up in our $7\ M_\odot$ model with initial metallicity $Z = 10^{-4}$. We focus our study on the impact of two convective boundary mixing parameters: $f_{\rm PDCZ}$—the f value characterising the mixing at the base of the pulse-driven convection zone—and $f_{\rm env}$—the equivalent value for the base of the convective envelope including during its penetration following the thermal pulse (TDU). The results of these models are summarised in Table 3. Initially, we continued the computation of the model holding our original assumption for the convective boundary mixing scheme ($f_{\rm env} = 0.0035$, $f_{\rm PDCZ} = 0.002$; see Section 2.2) and found that the model indeed encountered a situation whereby protons from the convective envelope were ingested into the PDCZ. This He-shell flash H-ingestion is different

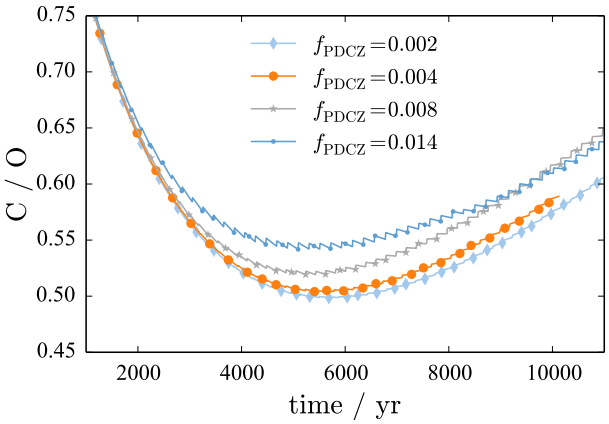


Figure 7. C/O ratio (C/O = $16X(^{12}\mathrm{C})/12X(^{16}\mathrm{O})$) at the stellar surface for the series of models with $M = 7\ M_\odot$ and $Z = 10^{-4}$ in which $f_{\rm env} = 0.0035$ and $f_{\rm PDCZ}$ is increased from 0.002 through 0.014 (first 4 models in Table 3).

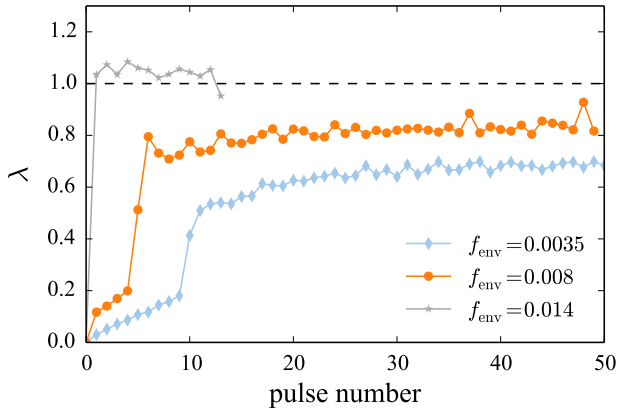


Figure 8. TDU efficiency λ for the series of models with $M = 7\ M_\odot$ and $Z = 10^{-4}$ in which $f_{\rm PDCZ} = 0.002$ and $f_{\rm env}$ is increased from 0.0035 through 0.014 (first entry and middle three entries in Table 3). Model with $f_{\rm env} = 0.022$ is actually not shown because it does not experience any TP events.

than the equivalent event in low metallicity low- and intermediate-mass stars (Fujimoto, Ikeda & Iben 2000; Herwig 2003a; Suda et al. 2004; Campbell & Lattanzio 2008; Cristallo et al. 2009), or H-deficient post-AGB stars (Herwig et al. 2011). In those situations, the hydrogen-burning shell separating the hydrogen-rich and helium-rich material is either weak or completely inactive. The entropy barrier is thus weaker and it is easier for the PDCZ to ingest protons. In super-AGB stars where dredge-up is hot (i.e. the hydrogen-burning shell is still active), it is much more difficult for the PDCZ to simply engulf some of the hydrogen-rich material in the same way. Instead, the combination of effects from the CBM below the PDCZ and the CBM below the convective envelope can be enough, in our current parameterisations, to initiate a convective-reactive event.

3.3.1 *Fixed $f_{\rm env}$*

Fixing the value of f parameter at the base of the envelope at our original assumption of $f_{\rm env} = 0.0035$ (see above), $f_{\rm PDCZ}$ was increased through the range 0.002–0.014. The impact on the TDU efficiency λ and the time between the onset of TDU and extinguishing of the PDCZ is shown in the bottom panel of Fig. 6. The peak He-burning luminosity during the shell flash is higher for larger values of $f_{\rm PDCZ}$. As a result the TDU begins sooner (Fig. 6, top panel) and becomes more efficient (Fig. 6, bottom panel). All of the models in this series experience H-ingestion during the TP-SAGB. Once this begins to occur, it becomes rather difficult to define at which point the PDCZ has extinguished. It is for this reason that only up to the 20$^{\rm th}$ pulse is plotted in the top panel of Fig. 6.

The peak hydrogen-burning luminosity $L_{\rm H}$ is given for each model in Table 3 (first 4 entries). All of the models encounter at least one thermal pulse with $L_{\rm H} > 10^9\ L_\odot$ and in the case with the largest extent of CBM ($f_{\rm PDCZ} = 0.014$) the H-burning luminosity even exceeds $10^{10}\ L_\odot$. That case is also unique because it is the only model in the series that mixes material up from the CO (He-free) core into the PDCZ during the He shell flash. This begins to happen at around pulse number 40. The C/O ratio for these four models as a function of evolutionary time is shown for the TP-SAGB phase in Fig. 7. The dredge-up efficiency is greater than unity for only the model with $f_{\rm PDCZ} = 0.014$, indicating that for such a parameterisation of the CBM below the pulse-driven convection zone the CO core will not grow to the critical mass for electron-captures to trigger its collapse.

3.3.2 *Fixed $f_{\rm PDCZ}$*

A second series of models was computed in which we fixed the value of the f parameter below the PDCZ at our initial assumption of $f_{\rm PDCZ} = 0.002$ and increased $f_{\rm env}$ through the range 0.0035–0.022. For the model with the largest value of the parameter ($f_{\rm env} = 0.022$) no thermal pulses were encountered. Instead the hydrogen-burning shell corrosively burned into the H-free core and, eventually, into the CO core (Herwig 2004a,b). With $f_{\rm env} = 0.014$, hydrogen ingestion and efficient TDU with $\lambda > 1$ are found frequently from the second thermal pulse onwards (see Fig. 8). A summary of this series of models is provided in Table 3 (first entry and middle 3 entries).

3.3.3 *Combined effect of $f_{\rm env}$ and $f_{\rm PDCZ}$*

In a final series of models we increased both $f_{\rm PDCZ}$ and $f_{\rm env}$ in tandem (last 4 entries in Table 3). The models behave as predicted based on our individual parameter studies for each parameter. The combined effects of the CBM below the PDCZ and the hot-bottom burning H envelope cause the model to experience H-ingestion TPs very early in the TP-SAGB phase (within the first 20 TPs). The model with $f_{\rm env} = 0.014$ and $f_{\rm PDCZ} = 0.014$ experiences the highest H-burning luminosity of all the models computed for this study: 2.31×10^{10} L$_\odot$. Fig. 9 shows a Kippenhahn (convective structure evolution) diagram of this most extreme H-ingestion super-AGB thermal pulse including contours of nuclear energy generation in the range $1 - 10^{16}$ erg g^{-1} s^{-1} for the model with $f_{\rm PDCZ} = 0.014$ and $f_{\rm env} = 0.014$. The model predicts energy generation rates from hydrogen combustion in excess of 10^{15} erg g^{-1} s^{-1}. The abundance profiles at this time are shown along with the temperature (top panel) and entropy (bottom panel) stratifications in Fig. 10. The model was computed for only 14 thermal pulses, however the value of the H-number (Eq. 3) during the second thermal pulse in this case was $H \approx 1.1$. This suggests that the amount of energy being released in the ingestion event is likely at least 10% greater than the internal energy of the material residing at the location where the energy is being released. If the CBM parameter choice is appropriate then the 1D hydrostatic stellar evolution assumptions are violated and the calculated results are indicative at best (see Section 4). For

$f_{\rm PDCZ}$	$f_{\rm env}$	comments on H ingestion events	peak $L_{\rm H}$ / $10^9 L_\odot$	λ
0.002	0.0035		8.26	< 1
0.004	0.0035		3.98	< 1
0.008	0.0035		4.35	< 1
0.014	0.0035	PDCZ mixes up some CO core	17.4	> 1
0.002	0.008		6.06	< 1
0.002	0.014	Only 14 pulses computed	3.87	> 1
0.002	0.022	No TP. H shell corrosively burns into CO core	–	–
0.004	0.008		7.47	< 1
0.008	0.014	Only 13 pulses computed, PDCZ mixes up some CO core	5.84	> 1
0.014	0.014	Only 14 pulses computed, PDCZ mixes up some CO core; one pulse is shown in Fig. 9	23.1	> 1
0.014	0.022	No TP. H shell corrosively burns into CO core	–	–

Table 3. Key properties of the models from the mixing parameter study at $Z = 10^{-4}$ with $M_{\rm ini} = 7\,M_\odot$. Aside from the models where no thermal pulses (TPs) occur, all of the models listed here experience H-ingestion events. $f_{\rm PDCZ}$ is the convective boundary mixing parameter f (Eq. 2) below the pulse driven convection zone and $f_{\rm env}$ is the parameter at the base of the convective envelope. The peak value of the H-burning luminosity is given in units of 10^9 $L_\odot$ and whether the TDU efficiency λ is greater or less than unity is given in the final column.

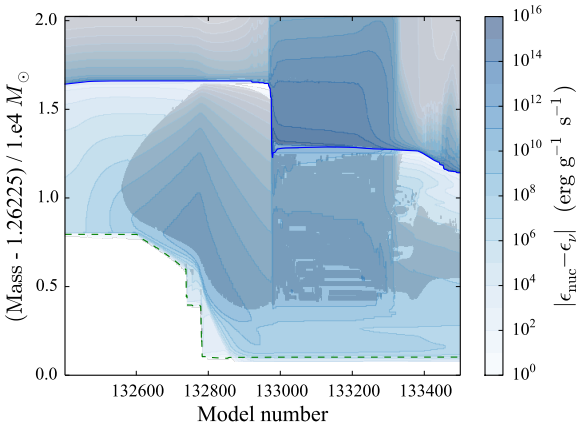


Figure 9. Evolution of the convective structure and nuclear energy generation during a thermal pulse in which hydrogen is ingested into the pulse-driven convection zone (PDCZ). The model shown here had initial mass $7\,M_\odot$ and metallicity $Z = 10^{-4}$ and was computed with $f_{\rm env} = 0.014$ and $f_{\rm PDCZ} = 0.014$ (penultimate model in Table 3). The regions shaded in grey are convectively unstable and the blue contours show regions of nuclear energy generation. The solid blue line marks the boundary above which the mass fraction of hydrogen is greater than 10^{-6} and the dashed green line marks the edge of the CO core. The ingestion event occurs around model number 133000, at which time profile plots of the important quantities are given in Fig. 10.

example, such strong energy release will certainly affect the hydrodynamic flow which will feed back into the ingestion event.

4 CONSEQUENCES OF HYDROGEN INGESTION DURING DREDGE-OUT AND THE TP-SAGB

We have identified in Section 3 two potential sites of H-ingestion in super-AGB stars and failed massive stars. These are stars that experience either dredge-out, He shell-flash thermal pulses or both. In the dredge-out, the region of convective instability associated with the He-burning shell grows outwards in mass and eventually coalesces with the convective envelope. This allows for the transport of protons down to He-burning temperatures on a convective timescale, where ^{12}C has been produced from He burning. Introducing protons to an environment rich in ^{12}C at temperatures of $\gtrsim 1.5 \times 10^8$ K results in a very rapid release of energy from H-^{12}C combustion (see also Gil-Pons & Doherty 2010).

Along the TP-SAGB, our models (assuming $f_{\rm PDCZ} = 0.002$ and $f_{\rm env} = 0.0035$; see Section 2) suggest that super-AGB stars with a wide range of initial metallicities ($10^{-5} \leqslant Z \leqslant 0.02$) evolve towards the conditions required for an exchange of material between the pulse-driven convection zone (PDCZ) and the convective hydrogen envelope. Such a direction of evolution involves: (i) the shortening of the time between the end of the PDCZ and the onset of the third dredge-up (TDU) into the intershell and (ii) the increasing of the efficiency of the TDU, λ.

4.1 Validity of the 1D approximation

From our simulations of dredge-out in TP-SAGB stars—which are spherically symmetric models in hydrostatic equilibrium computed using the MESA code and holding the assumptions described in Section 2—we have calculated the H-number (Eq. 3) for the time when the H-^{12}C combustion is most energetic. This number is an estimation of the amount of energy released over one convective turnover time scale in units of the local internal energy of the stellar material. During dredge-out in an 8.4 $M_\odot$ stellar model with an initial metallicity of $Z = 0.01$ we find a lower limit of $H = 0.11$. During a thermal pulse of a 7 $M_\odot$ super-AGB star model with an

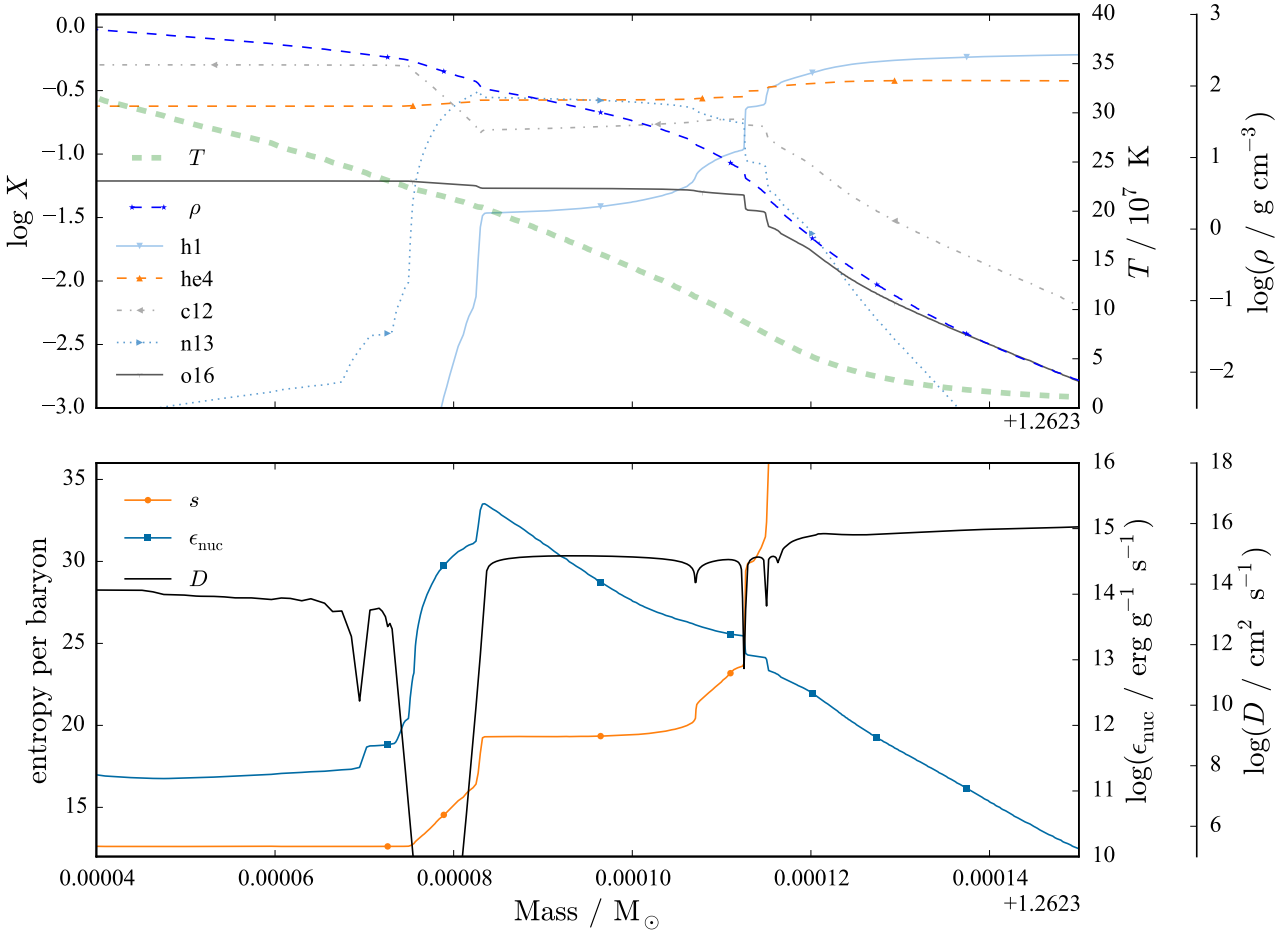


Figure 10. Abundance profiles, temperature and density (top panel) and entropy s, specific rate of nuclear energy generation and diffusion coefficient (bottom panel) in the 7 $M_\odot$ $Z = 10^{-4}$ model during the peak energy generation due to H-^{12}C combustion (around model 133000 in Fig. 9). In this model, the convective boundary mixing parameters at the bottom of the PDCZ and at the bottom of the envelope were $f_{\rm PDCZ} = 0.014$ and $f_{\rm env} = 0.014$, respectively (see penultimate entry in Table 3.

initial metallicity of $Z = 10^{-4}$ and convective boundary mixing parameters $f_{\rm PDCZ} = 0.002$ and $f_{\rm env} = 0.014$ we estimate that $H \approx 1.1$. Such conditions will certainly feed back into the hydrodynamic flow of the stellar material, which in turn will feed back into the entrainment and burning rates (Herwig et al. 2014).

As we describe in Section 3, after some time in our 1D calculations the ingestion episode is quenched. This means that the flow of protons from the H-rich convective envelope into the convective He-burning layer is choked off by the formation of an entropy barrier. The formation of such an entropy barrier arises because the protons burn as they are diffused inwards, down toward higher temperatures. The time scales of mixing, burning and nuclear energy generation are similar to one another. Under these conditions, it is questionable whether the mixing length theory of convection (MLT) can provide the correct solution for the transport of entropy and nuclear species. The behaviour of H-ingestion events would be characterized by: how many protons are mixed into the ^{12}C-rich layer, how far in are they transported and where is the energy from H-^{12}C combustion deposited. For this, 3D simulations are necessary (see, e.g., Herwig et al. 2011; Stancliffe et al. 2011; Herwig et al. 2014, for similar examples of H-ingestion in low-metallicity AGB stars and post-AGB stars).

4.2 Mass ejection and transients triggered by proton-ingestion

The simulations by Herwig et al. (2014) suggest that H-ingestion into ^{12}C-rich He-shell convection can trigger a non-radial instability, the global oscillation of shell H-ingestion (GOSH). It is conceivable that a GOSH instability in a violent proton-ingestion event in a super-AGB star could drive an outburst that rises through the star and is ejected in a pre-supernova explosion. At the shell, temperatures can reach in excess of 2×10^8 K. These outbursts could have implications for multiple classes of "supernova" explosions, both as precursors of narrow-line supernovae and, as possible in explanations of specific peculiar subclasses of supernovae. Although the thorough study needed to determine the viability of these outbursts in explaining these subsclasses is beyond the scope of this paper, in this section we conduct a first look at the transient properties of these outbursts.

First and foremost, the mass ejecta from these outbursts can

produce the circumstellar debris needed to explain type IIn supernovae. Observations of type IIn supernovae are providing a growing list of properties of the circumstellar medium surrounding these supernova explosions (e.g. Miller et al. 2010; Kankare et al. 2012; Fox et al. 2013; Ofek et al. 2014; Moriya & Maeda 2014; Taddia et al. 2013). Ofek et al. (2014) argue that over half of all type IIn supernova have precursors within 1/3 yr of the supernova explosion with masses exceeding 0.001 $M_{\odot}$. Moriya & Maeda (2014) instead argue that the IIn supernovae in their sample are fit by enhanced mass loss rates of $10^{-3} - 1\ M_{\odot}\ \mathrm{yr}^{-1}$ for 5 – 60 years prior to the explosion with total ejecta masses lying between $0.01 - 10\ M_{\odot}$. Miller et al. (2010) argued that dense clumps exist as far out as 1.7×10^{16} cm. For most of these shell-burning outbursts, the explosion occurs too long before collapse to produce an observed signal in the supernova light-curve. However, in some cases, our models can produce the observed IIn CSM distributions.

Corsi et al. (2014) and Gal-Yam et al. (2014) have seen evidence of outbursts at the few year time-frame even for supernova not of the type IIn subclass, the primary difference being the ejecta is smaller and the outburst happened longer prior to the supernova explosion. These explosions may also be an indicator of helium-shell proton-ingestion outbursts. To predict the shape of the light curve that could be produced during the ejection of material caused by a proton ingestion event occurring deep within the star, we mimic the outburst by assuming the hot material is ejected from the burning layer. As it rises through the star, it expands and cools adiabatically prior to bursting out of the stellar surface. We assume that the drive from the burning layer only allows the ejecta to expand laterally, and the volume of the ejecta increases as the square of its position until it is ejected from the star. Using the temperature at the burning layer, and assuming adiabatic expansion, we can calculate the thermal energy of the ejecta as it breaks out of the star.

After the outburst breaks out of the star, we use a semi-analytic solution to calculate the light-curve of these explosions, assuming spherical symmetry and homologous outflow conditions (see Bayless et al. 2014, for details). To estimate the light-curve of these outbursts, we varied the energy ($10^{47} - 10^{49}$ erg), temperature ($1 - 3 \times 10^{8}$ K) and mass ($0.01 - 0.1\ M_{\odot}$) of this rising outburst. Figure 11 shows a range of light-curves estimated from this method. The calculations assume average escape velocity v_{ejecta} set to $(2E_{\mathrm{exp}}/M_{\mathrm{ejecta}})^{1/2}$ where M_{ejecta} is the ejecta mass. The magnitude of the light-curve depends sensitively on the thermal energy, but the duration of the burst can be altered by changing either the explosion energy or the mass, and without an accurate velocity measurement, it will be difficult to distinguish between these models.

Note that these outbursts lie somewhere between supernovae and novae and, for both small ejecta masses ($< 0.1\ M_{\odot}$) or energetic explosions, the duration is shorter than typical supernovae with rise/decay times on order of 10 days. Without more detailed calculations of the propagation of the burning episode through the star, it is difficult to constrain the light-curve further. These light-curves may explain the pre-explosion outbursts seen by Corsi et al. (2014) and Gal-Yam et al. (2014). Similar pre-SN outbursts and CSM production could be caused by the instability encountered in TP-SAGB stars described by Lau et al. (2012), should the entire envelope not be ejected and the star recover and evolve to an electron-capture supernova.

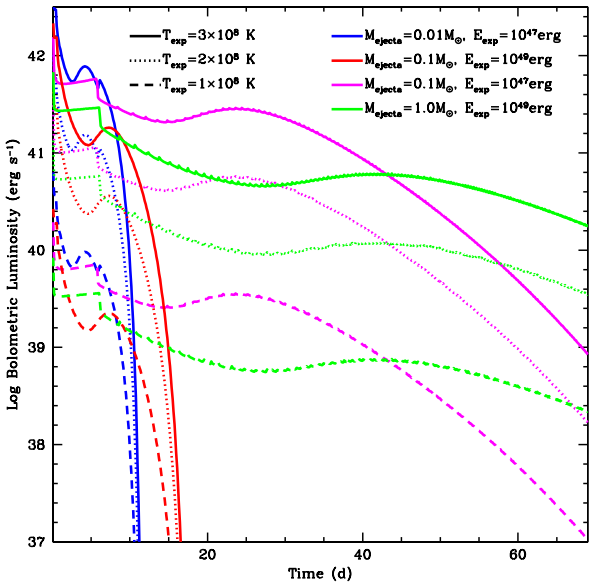


Figure 11. Bolometric light-curves of the possible signature from violent shell-burning explosions for different combinations of the shell burning temperature, ejected mass and the energy imparted to the ejected mass.

4.3 Neutron-capture nucleosynthesis and overabundance of n-capture products in ejected winds

H-^{12}C combustion produces ^{13}C, from which neutrons are then released via the $^{13}\mathrm{C}(\alpha, n)^{16}\mathrm{O}$ reaction. Given the right conditions during the hydrogen-ingestion event (abundance of protons, abundance of ^{12}C and the temperature), intermediate neutron densities of $N_n \approx 10^{15}$ cm^{-3} can be produced, defined as the *i* process by Cowan & Rose (1977, see Section 1).

i-process nucleosynthesis signatures are observed in young open clusters of the galactic disk (Mishenina et al. 2015) and may show up in galactic chemical evolution at lower metallicities, or in metal-poor mass-transfer binaries (Dardelet et al. 2015; Lugaro et al. 2012a; Cristallo et al. 2009). If low-metallicity super-AGB stars do indeed host the *i* process, then the corresponding signature may be found in globular cluster stars with strongly He-rich (second) generations (Herwig et al. 2012; Charbonnel et al. 2013; Karakas, Marino & Nataf 2014; Shingles et al. 2015).

However, unless we have performed a three-dimensional hydrodynamic simulation-based analysis of the interaction of nuclear burning and convective fluid-dynamic flow, we can not calculate the nucleosynthesis in the H-combustion dredge-up reliably based solely upon one-dimensional stellar evolution models (Herwig et al. 2011). In the meantime, we can explore a number of relevant questions that are independent of the hydrodynamic aspects. These are the enrichment of the envelope and ejecta of super-AGB stars (which will be presented in this section) and the general properties of nucleosynthesis at *i*-process conditions. Dardelet et al. (2015) presented one-zone nucleosynthesis simulations for typical *i*-process conditions, i.e. neutron densities of $N_{\mathrm{n}} \approx 10^{15}\mathrm{cm}^{-1}$. They have shown that the abundance pattern of some C-enhanced metal-poor stars classified as CEMP-s/r stars (carrying simultaneously the signature of elements usually associated with *s*-process and those associated with *r*-process; Beers & Christlieb 2005; Masseron et al. 2010; Bisterzo et al. 2012; Lugaro et al. 2012b) can be remarkably

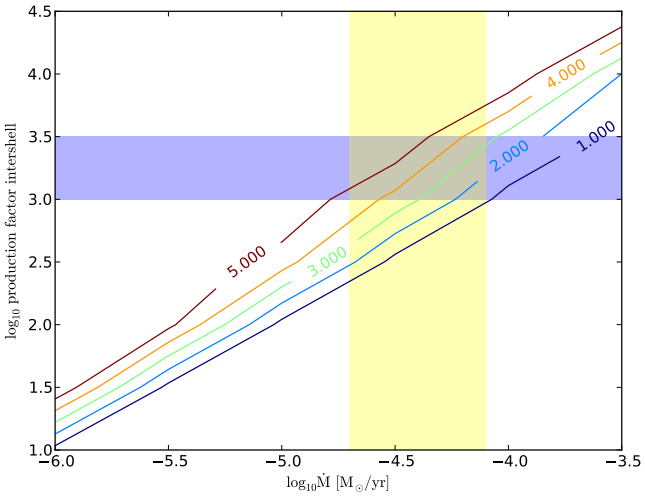


Figure 12. Estimate of n-capture overabundance in ejected winds of super-AGB thermal pulse stars with H-ingestion flash, as a function of stellar mass loss and n-capture production factor in the intershell. The lines are labelled with log of the overabundance in the ejecta; if the intial heavy element abundance was solar scaled the labels would numerically correspond to [s/Fe] where s stands for the average of n-capture elements produced. The range of observed mass loss rates in luminous M-type giants, supposedly massive AGB stars (van Loon et al. 2005) is shaded yellow. The n-capture production factor estimates (shown in blue, see text) are based on the detailed nucleosynthetic H-ingestion flash investigation by Herwig et al. (2011), and our *i*-process single-zone calculations (Dardelet et al. 2015).

well reproduced by one-zone simulations if the neutron exposure is used as a fitting parameter. If these preliminary results are confirmed in a more detailed investigation then H-ingestion events in super-AGB stars would be a possible site for the *i*-process observed in CEMP-s/r stars. The C enhancement in CEMP stars would then likely come from the C-rich He-shell layer of which a larger fraction would be mixed to the envelope and ejected during the violent non-radial instabilities associated with the H-ingestion flash (Herwig et al. 2014) that are in contrast with 1D stellar evolution models. The predictions for *i*-process simulations rely on nuclear physics data that is presently only available from theory (Bertolli et al. 2013). Experiments for unstable species involved in *i*-process simulations will have to be performed in the future to improve this situation.

In order for *i*-process nucleosynthesis from the SAGB hydrogen-ingestion thermal pulses to become observable, the nuclear production in the He-shell with H-ingestion needs to be high enough, and repeated events are needed to enrich the envelope before it is lost to the interstellar medium. One concern would be that the intershell in the super-AGB stars is so small in mass that even repeated exposure and dredge-up events may not lead to significant overabundances in the—at least initially—massive super-AGB envelopes. One possible scenario mentioned above involves a dynamic ejection of envelope material triggered by the energy input and instabilities induced by the H-ingestion flash. Alternatively, in the TP-SAGB case the enrichment of the envelope may proceed more gradually, one dredge-up event at at time.

Although the third dredge-up in some cases can be efficient in terms of the dredge-up parameter ($\lambda \approx 1$; see Section 3.3 and Figs. 6 and 8) the mass of the inter-shell region is only of the order $\approx 10^{-4}\,M_\odot$ (see Fig. 9). Even if large production factors can be regularly obtained in the inter-shell region, the large dilution into a massive super-AGB envelope may prevent large overabundance factors in the ejected materials.

We have constructed a simple mixing model to clarify this question. In our simulation with $f_{\rm env} = 0.014$ the core mass remains approximately constant due to efficient dredge-up after each thermal pulse. Thus, the total number of thermal pulses that the model could encounter would depend only on the mass loss rate for a given envelope mass. For $M_{\rm env} = 6\,M_\odot$ and an approximately constant interpulse time—because of the constant core mass with $\lambda \approx 1$—of $t_{\rm interp} \approx 782$ yr, a mass loss rate of $\log(\dot{M}/\,M_\odot\,{\rm yr}^{-1}) = -5$ (-4) translates into about 800 (about 80) thermal pulses. The overproduction factor can be estimated by evaluating the following simple mixing model:

$$s_{\rm env}^{\rm n+1} = s_{\rm IS}^{\rm n}\,\frac{f_{\rm enr} m_{\rm IS} + m_{\rm env}^{\rm n}}{m_{\rm IS} + m_{\rm env}} \quad (5)$$

$$m_{\rm s,eject}^{\rm n+1} = m_{\rm s,eject}^{\rm n} + s_{\rm env}^{\rm n+1} t_{\rm interp} \dot{M} \quad (6)$$

$$m_{\rm env}^{\rm n+1} = m_{\rm env}^{\rm n} - t_{\rm interp}\dot{M} \quad (7)$$

where $s_{\rm env}$ and $s_{\rm IS}$ are the heavy element abundances in the envelope and in the inter-shell respectively, $f_{\rm enr}$ is the production factor of heavy elements in the inter-shell, $m_{\rm env}$ and $m_{\rm env}$ are the mass of the envelope and the inter-shell respectively, $m_{\rm s,eject}$ is the mass of heavy elements in the wind ejecta, and $\dot{M}$ is the mass loss rate. The overabundance in the total wind ejecta is then $m_{\rm s,eject}^{\rm final}/m_{\rm env}^{\rm inital}$, and corresponds to [s/Fe] if s has the solar-scaled value in the initial abundance. This overabundance is shown in Fig. 12 as a function of assumed mass loss rate and inter-shell production factors, assuming an average inter-shell mass of $m_{\rm IS} = 7\times10^{-5}\,M_\odot$ and an initial envelope mass of $6\,M_\odot$.

Some guidance on the expected production factors of the vigorous H-ingestion/He-shell flash encountered in the super-AGB thermal pulses may be gained from the related situation in post-AGB H-ingestion flash models representing Sakurai's object (Herwig et al. 2011). There, production factors of about 100 were found for an individual event, although limited to the first-peak elements. The initial metallicity of our simulation with $f_{\rm env} = 0.014$ is $Z = 10^{-4}$ and therefore the production might be more efficient for heavier elements, since the neutron source is primary. Consistent with the lower initial abundances, the logarithmic production factors in the inter-shell may be in the range $3 - 3.5$ after each H ingestion event (see marked range in Fig. 12).

We conclude that with an estimate of the super-AGB mass loss of $\log(\dot{M}/\,M_\odot\,{\rm yr}^{-1}) \approx -4.1$ and production factors of the order 1000 in the intershell, we expect overabundances of the heavy *i*-process elements in the wind ejecta of $1 - 2$ dex. Therefore, the *i*-process triggered by the $^{13}{\rm C}(\alpha,n)^{16}{\rm O}$ reaction may have a comparable or even larger efficiency with respect to the ^{22}Ne neutron source activated at the bottom of the convective TPs (Doherty et al. 2014). On the other hand, the $^{13}{\rm C}(\alpha,n)^{16}{\rm O}$ reaction is a much more efficient neutron source in producing heavier elements than $^{22}{\rm Ne}(\alpha,n)^{25}{\rm Mg}$. Indeed, the ^{22}Ne itself is also a relevant neutron poison and produces by the (α,n) channel another neutron poison in ^{25}Mg, reducing the neutron-capture efficiency beyond iron (see the behaviour of the ^{22}Ne as a neutron source in fast rotating massive stars and in low-mass AGB stars at low metallicity, Pignatari et al. 2013; Husti et al. 2007).

5 SUMMARY AND CONCLUSIONS

This paper describes two types of H-ingestion events arising in simulations of 7–10 $M_\odot$ stars. One type of event occurs in our

super-AGB (SAGB) stellar evolution simulations during the thermal pulse phase and the other occurs during the dredge-out phase in SAGB stars and some stars that ignite neon off-centre.

Our simulations of SAGB stars with initial metallicities in the range $10^{-5} \leqslant Z \leqslant 0.02$ include mixing processes at convective boundaries (CBM; Freytag, Ludwig & Steffen 1996; Herwig et al. 1997). All SAGB star models evolve during the thermal pulse phase toward conditions required for hydrogen-ingestion to occur during the He-shell flash. We suggest that this evolution is characterised by two main behaviours: (i) the efficiency of the penetration of the base of the convective envelope into the He intershell (third dredge-up, TDU; see §3.2) increases as the stars evolve along the thermal pulse phase and (ii) the TDU begins before the pulse-driven convection zone (PDCZ) has completely extinguished.

Hydrogen-ingestion thermal pulses occur in our SAGB stellar models for a large range of the CBM parameter f representing the mixing efficiency below the hydrogen envelope and below the PDCZ ($f_{\rm env}$ and $f_{\rm PDCZ}$, respectively). In particular, using the value of $f_{\rm PDCZ} = 0.008$ which has been shown to reproduce observational characteristics of post-AGB stars (Werner & Herwig 2006) and nova shell flashes (Denissenkov et al. 2013), we find hydrogen-ingestion thermal pulses to occur frequently for both $f_{\rm env} = 0.0035$ and 0.014 (and for values in-between). It is important to stress that both of these values of $f_{\rm env}$ are much lower than what is usually assumed for AGB stars (see, e.g., Lugaro et al. 2003). However, with dredge-up being hot in super-AGB stars one would expect a greater entropy barrier at the bottom of the convective hydrogen envelope than in low-mass AGB stars and thus a lower efficiency of CBM. Quite what the efficiency of the CBM is and hence, what an appropriate choice of the parameter f should be for the bottom of the convective envelope, is unclear at present. Our models suggest that for $f_{\rm env} \gtrsim 0.014$ the efficiency of the 3DUP λ will be greater than unity and thus the He-free core will not grow during the TP-SAGB. This scenario would therefore suggest a very low electron-capture supernova rate from super-AGB stars (see also Poelarends et al. 2008).

The dredge-out phase in massive super-AGB stars and some stars that ignite neon off-centre is another situation in which protons and ^{12}C are brought together under He-burning temperatures on a convective turnover time scale (see also Ritossa, García-Berro & Iben 1999; Siess 2007; Doherty et al. 2015). We have shown the results of a simulated dredge-out episode that indeed depicts precisely these conditions (see also Gil-Pons & Doherty 2010). The behaviour is less sensitive to CBM at the bottom of the convective hydrogen envelope in this scenario. Indeed, we have simulated the phenomenon by assuming no CBM takes place at all at this boundary and still the dredge-out occurs (in fact, several previously published SAGB stellar models depicting dredge-out do not include the effects of CBM, e.g. Siess 2007).

Our simulations are performed in spherical symmetry and employ the mixing length theory of convection with time-dependent mixing treated as a diffusion process. Under these assumptions, the protons burn as they diffuse inwards and form an entropy barrier that chokes off further transport of hydrogen into the hot, ^{12}C-rich layers. Whether such a spherically symmetric entropy barrier would form in a real star and whether it would completely inhibit the transport of protons into the ^{12}C-rich layers is an open question. However, similar conditions have been found in simulations of the very late thermal pulse (VLTP) in Sakurai's object (Herwig et al. 2011). In that case observations can be explained if it is assumed that such a barrier formation and prohibition of proton transport does *not* occur.

The H-combustion events we find in our models are vigorous, leading to significant mixing events that bring together protons and ^{12}C at He-burning temperatures. Detailed nucleosynthesis simulations for a related case, Sakurai's object, suggest that substantial production of trans-iron elements would likely occur in such H-ingestion events, and that the n-capture nucleosynthesis would proceed at a neutron density inbetween that of the *s* process and *r* process (Herwig et al. 2011). The simulation of these *i*-process conditions for Sakurai's object indicate a strong production of the first-peak elements, while Ba and La are not efficiently made, leading to a simulated second to first peak *s*-process-index ratio of [hs/ls]≈ -1.8, roughly in agreement with observations. Post-AGB stars have only a very small amount of about $10^{-4}\,M_{\odot}$ of H-rich envelope material left. This justified mixing assumptions that effectively limited the neutron exposure so that the observed abundance pattern of a large enhancement of first-peak but not second-peak elements could be reproduced.

In the H-ingestion thermal pulses of super-AGB star models with CBM an envelope with several solar masses of H-rich material remains. This, as well as the higher neutron to Fe seed ratio in low-Z stars, and the possibility of recurrent H-ingestion events in SAGB thermal pulses imply that H-ingestion events in SAGB stars could be a site for *i* process with higher neutron exposure. This would lead to large enhancements of second-peak elements as observed in some of the CEMP-s/r stars. In fact, preliminary studies indicated that some CEMP-s/r stars are indeed very well reproduced by *i*-process-nucleosynthesis (Dardelet et al. 2015). We therefore propose that *i* process in low-Z SAGB stars is a potential origin of some CEMP-s/r stars. Since hot bottom burning takes place in super-AGB stars, their envelopes are O-rich and not C-rich. If H-ingestion thermal pulse nucleosynthesis in super-AGB stars are responsible for a subset of the CEMP-s/r stars, the enrichment is probably coming from the ejection of intershell material during a dynamic response to the convective-reactive H-ingestion flash, such as a GOSH (see Herwig et al. 2014 and Section 4.2). Such outbursts would produce faint transients lying somewhere between supernovae and novae, and may explain a fraction of transient events that are observed shortly before a supernova explosion.

ACKNOWLEDGMENTS

This paper arose, in part, out of discussions early on with Don VandenBerg, to whom the authors are grateful.

SJ is a fellow of the Alexander von Humboldt Foundation. FH acknowledges funding through a Discovery Grant from NSERC. MP acknowledges support from the "Lendület-2014" Programme of the Hungarian Academy of Sciences (Hungary) and from SNF (Switzerland). MP is also thankful for support from EuroGENESIS. MGB's research is supported by the US Dept. of Energy, Office of Nuclear Physics. BP is supported by the NSF under grants PHY 11- 25915, AST 11-09174, and ACI 13-39581.

REFERENCES

Abia C. et al., 2002, ApJ, 579, 817

Anderson A. J., 1997, PhD thesis, University of California, Berkeley

Angulo C., Arnould M., Rayet, M. et al., 1999, Nucl. Phys., A 656, 3

Bayless A. J., Even W., Frey L. H., Fryer C. L., Roming P. W. A., Young P. A., 2014, ArXiv e-prints
Beers T. C., Christlieb N., 2005, Annual Review of Astronomy and Astrophysics, 43, 531
Bertolli M. G., Herwig F., Pignatari M., Kawano T., 2013, ArXiv e-prints
Bisterzo S. et al., 2015, MNRAS, 449, 506
Bisterzo S., Gallino R., Straniero O., Cristallo S., Käppeler F., 2012, MNRAS, 422, 849
Blöcker T., 1995, A&A, 297, 727
Campbell S. W., Lattanzio J. C., 2008, A&A, 490, 769
Campbell S. W., Lugaro M., Karakas A. I., 2010, A&A, 522, L6
Casanova J., José J., García-Berro E., Calder A., Shore S. N., 2011, A&A, 527, A5+
Caughlan G. R., Fowler W. A., 1988, Atom. Data Nucl. Data Tables, 40, 283
Charbonnel C., Chantereau W., Decressin T., Meynet G., Schaerer D., 2013, A&A, 557, L17
Chen M. C., Herwig F., Denissenkov P. A., Paxton B., 2014, MNRAS, 440, 1274
Chen M. C., Herwig F., Denissenkov P. A., Paxton B., 2014, Monthly Notices of the Royal Astronomical Society, 440, 1274
Corsi A. et al., 2014, ApJ, 782, 42
Cowan J. J., Rose W. K., 1977, ApJ, 212, 149
Cox J. P., Giuli R. T., 1968, Principles of stellar structure, Cox, J. P. & Giuli, R. T., ed.
Cristallo S., Piersanti L., Straniero O., Gallino R., Domínguez I., Käppeler F., 2009, Publications of the Astronomical Society of Australia, 26, 139
Cristallo S., Straniero O., Gallino R., Piersanti L., Domínguez I., Lederer M. T., 2009, ApJ, 696, 797
Dardelet L. et al., 2015, Proceedings of Nuclei in the Cosmos XIII, 7-11 July, 2014, Debrecen, Hungary
Delgado-Inglada G., Rodríguez M., Peimbert M., Stasińska G., Morisset C., 2015, MNRAS, 449, 1797
Denissenkov P. A., Herwig F., Bildsten L., Paxton B., 2013, ApJ, 762, 8
Denissenkov P. A., Herwig F., Truran J. W., Paxton B., 2013, The Astrophysical Journal, 772, 37
Denissenkov P. A., Tout C. A., 2003, Monthly Notices of the Royal Astronomical Society, 340, 722
Denissenkov P. A., Truran J. W., Herwig F., Jones S., Paxton B., Nomoto K., Suzuki T., Toki H., 2015, MNRAS, 447, 2696
Deupree R. G., 2000, ApJ, 543, 395
Doherty C. L., Gil-Pons P., Lau H. H. B., Lattanzio J. C., Siess L., 2014, MNRAS, 437, 195
Doherty C. L., Gil-Pons P., Siess L., Lattanzio J. C., Lau H. H. B., 2015, MNRAS, 446, 2599
Doherty C. L., Siess L., Lattanzio J. C., Gil-Pons P., 2010, MNRAS, 401, 1453
Farmer R., Fields C. E., Timmes F. X., 2015, ArXiv e-prints
Fox O. D., Filippenko A. V., Skrutskie M. F., Silverman J. M., Ganeshalingam M., Cenko S. B., Clubb K. I., 2013, AJ, 146, 2
Freytag B., Ludwig H. G., Steffen M., 1996, Astronomy and Astrophysics, 313, 497
Freytag B., Ludwig H.-G., Steffen M., 1996, A&A, 313, 497
Fujimoto M. Y., Ikeda Y., Iben, I. J., 2000, ApJ Lett., 529, L25
Gal-Yam A. et al., 2014, Nat., 509, 471
Garcia-Berro E., Iben, Jr I., Garcia-Berro, E, Garcia-Berro, E, 1994, The Astrophysical Journal, 434, 306
Gil-Pons P., Doherty C. L., 2010, MemSAI, 81, 974
Glasner S. A., Livne E., Truran J. W., 2012, MNRAS, 427, 2411
Goriely S., Siess L., 2004, A&A, 421, L25
Herwig F., 2000, Astronomy and Astrophysics, 360, 952
Herwig F., 2000, A&A, 360, 952
Herwig F., 2003a, in CNO in the Universe, ASP Conf. Ser. astro-ph/0212366
—, 2003b, in Stellar Rotation, ASP Conf. Ser. p. 000
—, 2004, ApJ, 605, 425
Herwig F., 2004a, ApJ, 605, 425
—, 2004b, ApJS, 651
Herwig F., Blöcker T., Schönberner D. S., El Eid M. F., 1997, A&A, 324, L81
Herwig F., Blöcker T. B., Driebe T., 2000, in The changes in abundances in AGB stars, D'Antona F., Gallino R., eds.
Herwig F., Freytag B., Fuchs T., Hansen J. P., Hueckstaedt R. M., Porter D. H., Timmes F. X., Woodward P. R., 2007, Why Galaxies Care About AGB Stars: Their Importance as Actors and Probes, 378, 43
Herwig F., Freytag B., Hueckstaedt R. M., Timmes F. X., 2006, ApJ, 642, 1057
Herwig F., Freytag B., Hueckstaedt R. M., Timmes F. X., 2006, ApJ, 642, 1057
Herwig F., Langer N., Lugaro M., 2003, The Astrophysical Journal, 593, 1056
Herwig F., Pignatari M., Woodward P. R., Porter D. H., Rockefeller G., Fryer C. L., Bennett M., Hirschi R., 2011, ApJ, 727, 89
Herwig F., VandenBerg D. A., Navarro J. F., Ferguson J., Paxton B., 2012, ApJ, 757, 132
Herwig F., Woodward P. R., Lin P.-H., Knox M., Fryer C., 2014, ApJL, 792, L3
Husti L., Gallino R., Bisterzo S., Cristallo S., Straniero O., 2007, MemSAI, 78, 523
Iglesias C. A., Rogers F. J., 1996, The Astrophysical Journal, 464, 943
Jones S. et al., 2013, ApJ, 772, 150
Kankare E. et al., 2012, MNRAS, 424, 855
Karakas A. I., Marino A. F., Nataf D. M., 2014, ApJ, 784, 32
Kromer M. et al., 2015, MNRAS, 450, 3045
Lau H. H. B., Gil-Pons P., Doherty C., Lattanzio J., 2012, A&A, 542, A1
Liu N., Gallino R., Bisterzo S., Davis A. M., Savina M. R., Pellin M. J., 2014, ApJ, 788, 163
Longland R., Iliadis C., Karakas A. I., 2012, Physical Reviews C, 85, 065809
Lugaro M., Campbell S. W., de Mink S. E., 2009, Publications of the Astronomical Society of Australia, 26, 322
Lugaro M., Herwig F., Lattanzio J. C., Gallino R., Straniero O., 2003, ApJ, 586, 1305
Lugaro M., Karakas A. I., Stancliffe R. J., Rijs C., 2012a, in American Institute of Physics Conference Series, Vol. 1484, American Institute of Physics Conference Series, Kubono S., Hayakawa T., Kajino T., Miyatake H., Motobayashi T., Nomoto K., eds., pp. 111–116
—, 2012b, ApJ, 747, 2
Lugaro M., Tagliente G., Karakas A. I., Milazzo P. M., Käppeler F., Davis A. M., Savina M. R., 2014, ApJ, 780, 95
Masseron T., Johnson J. A., Plez B., Van Eck S., Primas F., Goriely S., Jorissen A., 2010, Astronomy and Astrophysics, 509, A93
Mazzitelli I., D'Antona F., Ventura P., 1999, A&A, 348, 846
Meakin C. A., Arnett D., 2007, The Astrophysical Journal, 667, 448

Miller A. A. et al., 2010, MNRAS, 404, 305
Miller Bertolami M. M., Althaus L. G., Serenelli A. M., Panei J. A., 2006, Astronomy and Astrophysics, 449, 313
Mishenina T. et al., 2015, MNRAS, 446, 3651
Mocák M., Muller E., Siess L., 2011, ArXiv e-prints
Mocák M., Müller E., Weiss A., Kifonidis K., 2009, A&A, 501, 659
Moriya T. J., Maeda K., 2014, ApJL, 790, L16
Mowlavi N., 1999, A&A, 344, 617
Nomoto K., 1984, ApJ, 277, 791
—, 1987, ApJ, 322, 206
Ofek E. O. et al., 2014, ApJ, 789, 104
Paxton B., Bildsten L., Dotter A., Herwig F., Lesaffre P., Timmes F., 2011, ApJS, 192, 3
Paxton B. et al., 2013, ApJS, 208, 4
—, 2015, ArXiv e-prints
Piersanti L., Cristallo S., Straniero O., 2013, ApJ, 774, 98
Pignatari M. et al., 2013, ApJS submitted, arXiv:13076961, 1
Pignatari M. et al., 2013, ApJ, 762, 31
Poelarends A. J. T., Herwig F., Langer N., Heger A., 2008, ApJ, 675, 614
Ribas I., Jordi C., Gimenez A., 2000, MNRAS, 318, L55
Ritossa C., García-Berro E., Iben I. J., 1999, ApJ, 515, 381
Ritossa C., García-Berro E., Iben, Jr. I., 1999, ApJ, 515, 381
Rogers T. M., Glatzmaier G. A., Jones C. A., 2006, ApJ, 653, 765
Schroder K.-P., Pols O. R., Eggleton P. P., 1997, Monthly Notices of the Royal Astronomical Society, 285, 696
Shingles L. J., Doherty C. L., Karakas A. I., Stancliffe R. J., Lattanzio J. C., Lugaro M., 2015, MNRAS, 452, 2804
Siess L., 2007, A&A, 476, 893
—, 2010, A&A, 512, A10+
Siess L., Goriely S., Langer N., 2004, A&A, 415, 1089
Stancliffe R. J., Dearborn D. S. P., Lattanzio J. C., Heap S. A., Campbell S. W., 2011, ApJ, 742, 121
Straniero O., Cristallo S., Piersanti L., 2014, ApJ, 785, 77
Suda T., Aikawa M., Machida M. N., Fujimoto M. Y., Iben I. J., 2004, ApJ, 611, 476
Taddia F. et al., 2013, A&A, 555, A10
Tian C.-L., Deng L.-C., Chan K.-L., 2009, MNRAS, 398, 1011
Tkachenko A. et al., 2014, MNRAS, 438, 3093
van Loon J. T., Cioni M.-R. L., Zijlstra A. A., Loup C., 2005, A&A, 438, 273
Ventura P., D'Antona F., 2011, MNRAS, 410, 2760
Weiss A., Ferguson J. W., 2009, A&A, 508, 1343
Werner K., Herwig F., 2006, PASP, 118, 183
Woodward P., Herwig F., Porter D., Fuchs T., Nowatzki A., Pignatari M., 2008, in American Institute of Physics Conference Series, Vol. 990, First Stars III, pp. 300–308
Woodward P. R., Herwig F., Lin P.-H., 2015, ApJ, 798, 49
Woosley S. E., Heger A., 2015, ApJ, 810, 34
Zamora O., Abia C., Plez B., Domínguez I., Cristallo S., 2009, A&A, 508, 909